

# Resonant Excitation of Nonradial Modes in RR Lyr Stars

Rafał M. Nowakowski<sup>1</sup> and Wojciech A. Dziembowski<sup>1,2</sup>

<sup>1</sup> Nicolaus Copernicus Astronomical Center, ul. Bartycka 18, 00-716 Warsaw, Poland

e-mail: rafaln@camk.edu.pl

<sup>2</sup> Warsaw University Observatory, Al. Ujazdowskie 4, 00-478 Warsaw, Poland

e-mail: wd@astrouw.edu.pl

## ABSTRACT

We study a nonlinear development of radial pulsation instability to a resonant excitation of nonradial modes. Our theory covers the cases of axisymmetric ( $m=0$ ) modes as well as ( $m, -m$ ) pairs. Adopting a simplified treatment of the radial and nonradial mode coupling we find that the asymptotic state is a pulsation with constant amplitudes and we evaluate the relative amplitude of the nonradial component.

Observable consequence of the  $m=0$  mode excitation is a small period change and a more significant amplitude change, especially in the case of a dipole mode ( $l=1$ ). Such a mode has a fairly large excitation probability.

Significant amplitude and phase modulation is predicted in the case of excitation of a  $m=\pm 1$  pair. We suggest that this may explain Blazhko-type modulation in RR Lyr stars. If this model is correct, the modulation period is determined by the rotation rate and the Brunt-Väisälä frequency in the deepest part of the radiative interior.

*Stars: oscillations – Stars: variables: RR Lyr*

## 1 Introduction

Among a variety of types of pulsating stars, RR Lyr variables seem to be the most important ones. They are significant in various fields of astronomy: distance measurements, evolution of Population II and low mass stars, structure of Galaxy and, obviously, stellar pulsation theory. Thus, it is important to understand the nature of all phenomena connected with their pulsations. One can distinguish a few subclasses of RR Lyr stars: RRab stars pulsating in the fundamental radial mode with large amplitude; RRc stars – the first overtone pulsators with small amplitude and sinusoidal light curves; RRd stars that pulsate in both fundamental and first overtone modes.

The most intriguing phenomenon that has been waiting for theoretical explanation for almost a century is the Blazhko effect. It is characterized by periodic modulation of oscillation amplitude and phase on a longer time scale. The effect was discovered by Blazhko (1907). Basic properties of observed Blazhko-type modulations are summarized by Szeidl (1988) and Kovács (1993, 2000). According to these authors, about 20–30% of all RRab stars exhibit this phenomenon. The modulation is often quite strong, pulsation amplitude may change by a factor of up to 3 during the Blazhko cycle. Fourier analysis of light curves with the Blazhko effect shows two peaks, symmetrically spaced on both sides of the main

peak corresponding to the basic oscillation frequency, as well as similar peaks around harmonics of the main frequency. This feature of Fourier spectrum is by some treated as a definition of the phenomenon. However, we should stress that the Fourier analyses are not available for most of RRab stars reported to show the Blazhko effect.

Whether RRc stars exhibit this type of modulations was a matter of speculations for years. Recently such variables were discovered in the LMC by the MACHO project (see Kurtz *et al.* 2000, Alcock *et al.* 2000). However, incidence of the Blazhko phenomenon among RRc stars is much lower than in the RRab case and is estimated at about 2%.

Early explanations of the Blazhko effect postulated the existence of strong magnetic field with the axis inclined to the axis of rotation. This field was thought to cause a nonspherical distortion of the pulsation. Stellar rotation led to the amplitude modulation seen by observers. A mathematical model of magnetically modified pulsation was developed by Shibahashi (1995) (see also Shibahashi 2000). There are many basic problems connected with this model (see Kovács 1993, 2000) and we will not deal with it in this paper.

Alternative interpretations invoke nonlinear interactions between oscillation modes. Two approaches have been adopted: numerical simulations of fully-nonlinear pulsation and an approximate formalism of amplitude equations (AEs). The latter is the only available formalism for nonradial oscillations. It proved particularly useful to study effects of resonances (see *e.g.*, Dziembowski 1982, Buchler and Goupil 1984, Van Hoolst 1992, 1994). The AE-formalism finds its applications in various fields of physics. Our application bears most resemblance with work of Wersinger *et al.* (1980) who studied nonlinear interaction of plasma waves in the case of parametric resonance. These authors showed that solutions of AEs may be stationary (fixed-point), periodically modulated (periodic limit cycle) as a result of Hopf-bifurcation, or even chaotic. In the case of pulsating stars parametric resonance is likely responsible for limiting of oscillation amplitudes in  $\delta$ -Sct stars (Dziembowski and Królikowska 1985).

Moskalik (1986) proposed 2:1 resonance between the fundamental and the third overtone modes as a possible explanation of the Blazhko effect which would be a manifestation of the periodic limit cycle solution of the corresponding AEs. However, the values of parameters necessary to obtain modulated solutions seem to be outside the range of RR Lyr models (Kovács 1993 and references therein). Moreover, there is no sign of modulation in hydrodynamic simulations (Kovács and Buchler 1988).

Nowadays, the most promising hypotheses involve excitation of nonradial modes. Properties of such modes in giant pulsators (RR Lyr, Cepheids) were studied already over twenty years ago (Dziembowski 1977a, Osaki 1977) but until the early 90s these papers were largely out of interest of astronomers.

Van Hoolst (1992) derived AEs for resonance between two modes with nearly equal frequencies (the 1:1 resonance) in the adiabatic approximation. He calculated polytropic stellar model and found a nonradial mode with frequency close to that of the second radial overtone. For these two modes he calculated some parameters in AEs. For other parameters he considered wide ranges of

values. Depending on the values of parameters he found different types of solutions which include single mode pulsation, double mode pulsation with constant amplitudes, pulsation with periodically or chaotically modulated amplitudes.

Kovács (1993) and Van Hoolst and Waelkens (1995) proposed the 1:1 resonance between the radial fundamental mode and a nonradial mode as a possible explanation of the Blazhko effect. This type of resonance is not possible between low order radial modes. Van Hoolst *et al.* (1998, hereafter VDK) showed that in realistic RR Lyr models, nonradial mode spectra in the range of the fundamental and the first overtone radial modes are very dense. Hence the frequency distance between the radial and the nearest nonradial mode is very small. VDK studied stability of monomode radial pulsation in a representative RR Lyr star model. They found high probability of resonant excitation of the nonradial mode. The highest probability occurs for modes with  $l = 1, 5, 6$  and  $l = 1, 4$  at fundamental and first overtone modes, respectively. Dziembowski and Cassisi (1999, hereafter DC) repeated similar calculations for a set of realistic RR Lyr models covering the whole range of effective temperatures corresponding to instability strip in RR Lyr stars luminosity region and found that conclusions of VDK are generally valid. They found, in particular, that the probability of resonant excitation of nonradial modes is about 0.5, which is not far from the observed incidence rate of the Blazhko effect among RRab stars. According to their calculations, the effect should occur among first overtone pulsators nearly as often as among RRab stars, which is in a strong contradiction with observations. However, they stressed that excitation of a nonradial mode does not necessarily imply amplitude modulations.

Nonlinear consequences of nonradial mode excitation due to the 1:1 resonance have never been studied in application to RR Lyr stars. The Blazhko effect may be a manifestation of periodic limit cycle solution of AEs, but it may also be caused by nonradial mode excitation with constant amplitude. The latter possibility requires  $m \neq 0$ . In this case, the Blazhko period is related to but not identical with the rotation period.

In this paper we extend the formalism of AEs used by VDK to study solutions with finite amplitudes of nonradial modes. We keep simple scaling of resonant coefficients adopted by DC.

The plan of the paper is as follows. In Section 2 we outline the basic linear properties of nonradial modes in evolutionary models of RR Lyr stars. The properties are described in details by VDK and DC. In Section 3 we transform AEs of VDK into the form used in further part of this paper, by adopting some simplifications, *e.g.*, above mentioned scaling of coefficients. We study stationary solutions and their stability in Section 4, as well as time dependent solutions and attractors in Section 5. Section 6 is devoted to estimating the mode amplitudes and period changes caused by the resonant interaction in all DC's models, as well as the observational effect of  $m=0$  mode presence. In Section 7 we explain how the  $(m, -m)$  pair excitation may cause the observed amplitude and phase modulation. Section 8 includes conclusions and discussion of the results.

## 2 Nonradial Modes in RR Lyr Models

RR Lyr stars are Horizontal Branch helium burning giants, characterized by strong mass concentration in the center. VDK showed that in such stars the oscillation equations can be solved analytically in the deep interior, using an asymptotic approximation. The solution may be matched to the numerical solution in the envelope. Applying this procedure one can determine basic properties of nonradial modes. The most important is that there is always dense spectrum of nonradial modes near the two lowest degree radial mode frequencies. For a given  $l$ , the mode frequency decreases with increasing  $n$ . This is so because, owing to very high values of the Brunt-Väisälä frequency in the interior, all nonradial modes are in fact  $g$ -modes of high degree. When rotation is ignored all modes with the same  $l, n$  have the same frequency. Non-zero rotation means still denser spectrum for each  $l$ . In the envelope nonradial modes closest in frequency to a given radial mode have their radial eigenfunctions almost the same as the radial mode eigenfunctions. This remains true as long as the mode frequency is much higher than the Lamb frequency ( $L_l = c(l+0.5)/r$  where  $c$  is the local sound velocity).

Radial modes are of course purely acoustic and they propagate only in the envelope, where the Brunt-Väisälä frequency is lower than their eigenfrequencies. The outer layers determine properties of radial modes and the interior plays no role.

From linear nonadiabatic calculations we find time dependence of perturbations in the form  $\exp(i\omega_j + \kappa_j t)$  where  $\omega_j$  is the eigenfrequency and  $\kappa_j$  is the linear growth rate of mode numbered by  $j$ . The growth rate may be expressed as (see *e.g.*, Unno *et al.* 1989)

$$\kappa_j = \frac{W_j}{2I_j\omega_j} \quad (1)$$

where  $I_j$  is the inertia of the mode and  $W_j$  is the work integral, *i.e.*, the integral over star's volume of nonadiabatic operator acting on the eigenfunction. In the case of the radial mode it is enough to integrate over the envelope, because the contribution from the deep interior is negligible. In the case of the nonradial modes one may calculate separately the integrals over the deep interior (gravity waves propagation zone) and over the envelope (acoustic waves propagation zone). Moreover, the eigenfrequencies of both modes are nearly the same, and one can put  $\omega_0$  instead of  $\omega_l$  in the formula for the nonradial mode growth rate. With above assumptions one obtains

$$\kappa_0 = \frac{W_0}{2I_0\omega_0}, \quad (2)$$

$$\kappa_l = \frac{W_0 + W_g}{2I_l\omega_0} \equiv \kappa_{l,0} + \kappa_g. \quad (3)$$

The quantity  $\kappa_g = W_g/(2I_l\omega_0)$ , which is always negative, measures the damping rate in the deep interior.

DC calculated three sets of evolutionary models of RR Lyr stars (for different masses and metallicities). They used the procedure described by VDK for

these models and calculated properties of the two lowest radial modes and the corresponding resonant nonradial modes for a few lowest  $l$ 's. In the vicinity of the fundamental mode frequency, nonradial modes with  $l \geq 7$  are damped very strongly and they are never excited due to 1:1 resonance with the radial mode. The same is true for the modes with  $l \geq 6$  in the vicinity of the first overtone frequency.

In all numerical calculations in this paper we use data for models from DC.

### 3 Amplitude Equations

The amplitude equations used in this paper are based on those derived by Van Hoolst (1994) and used by VDK in their study of stability of radial pulsation in RR Lyr stars. Here we first derive our simplified form for the case of resonant coupling between a radial ( $l=0$ ) and an axisymmetric nonradial mode ( $l > 0, m=0$ ). Then we will derive corresponding equations for the case of coupling to a nonradial mode pair of the same degrees  $l$  and opposite azimuthal degrees,  $m$  and  $-m$ . We will see that there are no essential differences between these two cases. Some details of the derivation are deferred to Appendix A.

We introduce complex pulsation amplitudes  $\tilde{a}$  associated with an individual oscillation mode ( $j$ ), which are defined by the following expression for the displacement

$$\frac{\delta \mathbf{r}}{r_0} = \boldsymbol{\xi}_j(\mathbf{r}, t) = \frac{1}{2} \tilde{a}_j e^{i\omega_j t} \mathbf{w}_j(\mathbf{r}) + cc, \quad (4)$$

where  $r_0$  is the Lagrangian radial coordinate,  $\mathbf{w}_j$  is vector eigenfunction, and  $\omega_j$  is eigenfrequency of the mode. We adopt normalization

$$w_{j,r} = Y_{l_j, m_j} \sqrt{4\pi} \quad (5)$$

at the surface, which implies that  $|\tilde{a}|$  is the *rms* amplitude of the surface radius.

#### 3.1 The $m=0$ Case

The time dependence of amplitudes  $a_j = \tilde{a}_j \exp(i\omega_j t)$  is described by AEs. For the 1:1 resonance between the radial mode and axisymmetric nonradial mode the relevant AEs are (VDK)

$$\begin{aligned} \frac{da_0}{dt} &= (\kappa_0 + i\omega_0)a_0 + S_0^0 a_0 |a_0|^2 + S_0^l a_0 |a_l|^2 + \\ &\quad + R_0^1 a_0^* a_l^2 + R_0^2 a_l |a_l|^2, \end{aligned} \quad (6)$$

$$\begin{aligned} \frac{da_l}{dt} &= (\kappa_l + i\omega_l)a_l + S_l^0 a_l |a_0|^2 + S_l^l a_l |a_l|^2 + \\ &\quad + R_l^1 a_l^* a_0^2 + R_l^2 |a_l|^2 a_0 + R_l^3 a_l^2 a_0^*, \end{aligned} \quad (7)$$

where  $S_j^k, R_j^k$  denote saturation and resonant coupling coefficients, respectively. For odd  $l$  coefficients  $R_0^2, R_l^2$  and  $R_l^3$  vanish. In our work we devote special

attention to the case of  $l=1$  and thus we neglect all the terms involving these coefficients. We believe that application of so simplified system to even  $l$ 's will not result in large error because these terms are of higher order in the amplitude of the nonradial modes. We will see that the amplitudes of  $l > 1$  modes are always much smaller than that of the radial mode. We can now introduce real amplitudes  $A_j$  and phases  $\phi_j$  in the form  $a_j = A_j \exp(i\omega_j t + \phi_j)$  and separate Eqs. (6) and (7) into the real and the imaginary parts. This yields

$$\begin{aligned} \frac{dA_0}{dt} &= \left[ \kappa_0 + \Re(S_0^0)A_0^2 + \Re(S_0^l)A_l^2 + \right. \\ &\quad \left. + (\Re(R_0^1)\cos\Gamma - \Im(R_0^1)\sin\Gamma)A_l^2 \right] A_0, \end{aligned} \quad (8)$$

$$\begin{aligned} \frac{dA_l}{dt} &= \left[ \kappa_l + \Re(S_l^0)A_0^2 + \Re(S_l^l)A_l^2 + \right. \\ &\quad \left. + (\Re(R_l^1)\cos\Gamma + \Im(R_l^1)\sin\Gamma)A_0^2 \right] A_l, \end{aligned} \quad (9)$$

$$\begin{aligned} A_0 \frac{d\phi_0}{dt} &= \left[ \Im(S_0^0)A_0^2 + \Im(S_0^l)A_l^2 + \right. \\ &\quad \left. + (\Re(R_0^1)\sin\Gamma + \Im(R_0^1)\cos\Gamma)A_l^2 \right] A_0, \end{aligned} \quad (10)$$

$$\begin{aligned} A_l \frac{d\phi_l}{dt} &= \left[ \Im(S_l^0)A_0^2 + \Im(S_l^l)A_l^2 + \right. \\ &\quad \left. + (-\Re(R_l^1)\sin\Gamma + \Im(R_l^1)\cos\Gamma)A_0^2 \right] A_l, \end{aligned} \quad (11)$$

where we introduced the relative phase,

$$\Gamma \equiv 2(\Delta\omega t + \phi_l - \phi_0), \quad (12)$$

and the detuning parameter,  $\Delta\omega \equiv \omega_l - \omega_0$ . The time derivatives of the phases  $\phi_j$  give nonlinear corrections to the linear mode frequencies. Terms with saturation coefficients in Eqs. (10) and (11) give nonresonant corrections and may be neglected because they move the whole spectrum of nonradial modes without significant change of frequency distance between consecutive nonradial modes. Moreover, we assume that the resonant coupling coefficients may be regarded purely imaginary as in the adiabatic case (Van Hoolst 1992). Although pulsation is never strictly adiabatic, we follow here a suggestion of VDK who argued that real parts of these coefficients are much smaller than imaginary parts.

All coupling coefficients are proportional to the complicated integrals containing products of four eigenfunctions for the modes involved. These integrals can be separated into integrals over radial and angular coordinates. The latter are easy to calculate analytically, because they contain well known spherical harmonics. The former are not possible to be determined analytically. Nevertheless, some useful relations between coefficients can be derived. This is due to the fact that the radial eigenfunctions of both radial and nonradial modes are almost the same in the outer layers and integration of products of different eigenfunctions gives the same result. In Appendix A.1 it is found, in particular, that

$$S_0^l = 2S_0^0, \quad S_l^l = H_l S_l^0, \quad (13)$$

where  $H_l = \int_{-1}^1 \tilde{P}_l^4(x) dx$  and  $\tilde{P}_l^4$  is normalized Legendre polynomial. The values of  $H_l$  for a few low  $l$ 's are given in Table 1.

Table 1  
Numerical values of  $H_l$

$l$	$H_l$
1	0.9
2	1.071
3	1.180
4	1.260
5	1.322
6	1.373

Like the growth rates (see Eqs. 2 and 3), all the coupling coefficients are proportional to the inverse of mode inertia. Thus, they satisfy the relations

$$\frac{\Re(S_0^0)}{\kappa_0} = \frac{\Re(S_l^0)}{2\kappa_{l,0}} \equiv -\alpha, \quad (14)$$

$$\frac{\Im(R_0^1)}{\kappa_0} = \frac{\Im(R_l^1)}{\kappa_{l,0}} \equiv R. \quad (15)$$

Let us note that  $\alpha$  determines the amplitude of single-mode radial pulsation.

When we introduce the dimensionless time  $\tau \equiv \kappa_0 t$ , the dimensionless frequency distance  $\Delta\sigma \equiv \Delta\omega/\kappa_0$ , and the following quantities

$$\gamma \equiv -\frac{\kappa_g}{\kappa_{l,0}}, \quad I \equiv \frac{I_0}{I_l} = \frac{\kappa_{l,0}}{\kappa_0}, \quad (16)$$

we can, with the help of Eqs. (2), (3), (14), and (15), rewrite Eqs. (8)–(11) in the form

$$\frac{dA_0}{d\tau} = [1 - \alpha(A_0^2 + 2A_l^2) - R \sin \Gamma A_l^2] A_0, \quad (17)$$

$$\frac{dA_l}{d\tau} = I [1 - \gamma - 2\alpha(A_0^2 + H_l A_l^2) + R \sin \Gamma A_0^2] A_l, \quad (18)$$

$$A_0 \frac{d\phi_0}{d\tau} = R \cos \Gamma A_l^2 A_0, \quad (19)$$

$$A_l \frac{d\phi_l}{d\tau} = IR \cos \Gamma A_0^2 A_l. \quad (20)$$

We neglected the real parts of the resonant coefficients and the imaginary parts of the saturation coefficients, as was explained above. From the last two equations and Eq. (12), with an additional assumption of non-zero values of both amplitudes, we obtain

$$\frac{d\Gamma}{d\tau} = 2 \left( \Delta\sigma + \frac{d\phi_l}{d\tau} - \frac{d\phi_0}{d\tau} \right) = 2 (\Delta\sigma + R \cos \Gamma (IA_0^2 - A_l^2)). \quad (21)$$

Eqs. (17), (18), and (21) form a complete set of equations and we will use them to study double-mode solutions. The equations are invariant under the transformation

$$(\Delta\sigma, \Gamma) \rightarrow (-\Delta\sigma, \pi - \Gamma). \quad (22)$$

Thus, we will restrict ourselves to  $\Delta\sigma \geq 0$ .

### 3.2 The $m \neq 0$ Case

Resonant interaction between radial and nonradial modes with nearly equal frequencies is only possible when the nonradial mode has azimuthal number  $m$  equal zero. In other cases, all resonant coupling coefficients vanish, as was shown by Van Hoolst (1994). Nevertheless, modes with  $m \neq 0$  can interact with a radial mode due to the resonance between the radial mode and a pair of nonradial modes of the same value of  $l$  and opposite values of  $m$ . Analogical situation of resonance between modes of rotationally split triplet  $l = 1$  is described by Buchler *et al.* (1995). The difference is that in our case the  $m = 0$  mode is replaced by the radial mode. These authors call this kind of resonance the 1:1:1 resonance but we think a more appropriate name is the 2:1+1 resonance. The reason is that the three frequencies satisfy the resonant condition  $2\omega_0 \approx \omega_m + \omega_{-m}$ .

The AEs for the above-mentioned type of resonance have the form given *e.g.*, by Buchler *et al.* (1995). The relations between coupling coefficients similar to those in the  $m = 0$  case are derived in Appendix A.2. The relative phase  $\Gamma$  in this case is given by

$$\Gamma = 2\Delta\omega t + \phi_- + \phi_+ - 2\phi_0 \quad (23)$$

where  $\Delta\omega = (\omega_- + \omega_+)/2 - \omega_0$ . Such a definition of  $\Gamma$  and  $\Delta\omega$  is consistent with the  $m = 0$  case. In further studies we will assume that rotation is slow and except for the linear eigenfrequencies it does not change the dynamical properties of the nonradial modes. The radial eigenfunctions of these modes are  $m$ -independent. Thus, we have a full symmetry between coefficients in equations for amplitudes and phases of both nonradial modes. This means, in particular, that

$$\kappa_- = \kappa_+ \equiv \kappa_l, \quad S_- = S_+ \equiv S_l, \quad R_- = R_+ \equiv R_l \quad (24)$$

where quantities with subscript  $l$  are the same as in the  $m = 0$  case. We stress that in the present case there is only one non-vanishing resonant coefficient also for even  $l$ 's. Similarly as in the  $m = 0$  case we introduce dimensionless quantities



and we obtain

$$\frac{dA_0}{d\tau} = [1 - \alpha (A_0^2 + 2A_-^2 + 2A_+^2) - 2R \sin \Gamma A_- A_+] A_0, \quad (25)$$

$$\frac{dA_-}{d\tau} = I [1 - \gamma - 2\alpha (A_0^2 + H_l^m (A_-^2 + 2A_+^2))] A_- + IR \sin \Gamma A_0^2 A_+, \quad (26)$$

$$\frac{dA_+}{d\tau} = I [1 - \gamma - 2\alpha (A_0^2 + H_l^m (2A_-^2 + A_+^2))] A_+ + IR \sin \Gamma A_0^2 A_-, \quad (27)$$

$$A_0 \frac{d\phi_0}{d\tau} = 2R \cos \Gamma A_- A_+ A_0, \quad (28)$$

$$A_- \frac{d\phi_-}{d\tau} = IR \cos \Gamma A_0^2 A_+, \quad (29)$$

$$A_+ \frac{d\phi_+}{d\tau} = IR \cos \Gamma A_0^2 A_-, \quad (30)$$

where  $H_l^m = \int_{-1}^1 \tilde{P}_{l,m}^A(x) dx$ ,  $\tilde{P}_{l,m}$  is normalized associated Legendre function and Eqs. (23) and (28)–(30) allow us to write equation for the phase  $\Gamma$

$$\frac{d\Gamma}{d\tau} = 2\Delta\sigma + R \cos \Gamma \left[ I A_0^2 \left( \frac{A_+}{A_-} + \frac{A_-}{A_+} \right) - 4A_- A_+ \right]. \quad (31)$$

Eqs. (25)–(27) together with Eq. (31) form a complete system of equations which allow us to determine the amplitudes of the modes participating in oscillations.

When we multiply Eq. (26) by  $A_-$ , Eq. (27) by  $A_+$ , and subtract them, we obtain

$$\frac{d}{d\tau} (A_-^2 - A_+^2) = 2I [1 - \gamma - 2\alpha A_0^2 - 2\alpha H_l^m (A_-^2 + A_+^2)] (A_-^2 - A_+^2). \quad (32)$$

It will be seen further that a typical value of  $A_0^2$  for stationary solutions is about  $1/\alpha$  (exact equality is for single-mode solution). This means negative value of the square bracket in Eq. (32) and exponential decrease of the difference of the two amplitudes. Thus, we limit ourselves to the  $A_- = A_+$  solution.

Let us now focus on the case of modes with  $l=1$ ,  $m=\pm 1$ . Then we have  $H_1^1 = 3/5$ . When we introduce a pseudo amplitude  $A_l$

$$A_- = A_+ \equiv \frac{A_l}{\sqrt{2}}. \quad (33)$$

then Eqs. (25)–(27) and (31) are identical with Eqs. (17), (18), and (21), where  $H_1 = 9/10$ . Thus, we may consider the pair of nonradial modes  $l=1$ ,  $m=\pm 1$  as an equivalent of the mode  $l=1$ ,  $m=0$ . This fact has a simple physical and geometrical explanation: spherical harmonic  $Y_{1,0}$  is equivalent to the sum of spherical harmonics  $Y_{1,-1} + Y_{1,1}$  divided by  $\sqrt{2}$  in the system of coordinates with the  $z$ -axis inclined by  $\pi/2$ . The pair of modes  $l=1$ ,  $m=\pm 1$  excited with the same amplitudes form a distortion of the star that has the same shape as the distortion associated with the mode  $l=1$ ,  $m=0$  but with the axis of

symmetry lying in the plane of equator. Since all physical mode characteristics are  $m$ -independent such a pair interacts with the radial mode in the same way as the  $l=1, m=0$  mode. Therefore, the amplitude  $A_l$  determined as a solution of Eqs. (17), (18), and (21) gives also the amplitudes of the nonradial modes  $A_{\pm} = A_l/\sqrt{2}$ .

We treat the interaction of the radial mode with the  $l=1, m=0$  mode and with the  $l=1, m=\pm 1$  pair independently. Strictly speaking this is justified only for the instability analysis. The small quadratic effects in the rotation rate cause that  $(\omega_{1,1} + \omega_{1,-1})/2 \neq \omega_{1,0}$  and these two cases are indeed independent. However, at finite amplitudes of the nonradial modes the interaction between the modes within the triplet is likely to be important. It is possible that the whole triplet will be excited but this should not have large consequences for amplitude prediction.

Similarity of the 1:1 and the 2:1+1 resonances, involving the  $(m, -m)$  doublet, extends to  $l > 1$ . The only difference concerns the  $H_l$  coefficient (see Eqs. 26 and 27).

It is also possible for a pair of nonradial modes belonging to different multiplets (*i.e.*, of different radial orders) to be excited. Then the amplitudes of the two modes cannot be assumed equal. The difference is mainly due to the difference in mode inertia, which is strongly frequency sensitive. We define  $I_{\pm}$  similarly as in Eq. (16), that is we set

$$I_{\pm} = \frac{I_0}{I_{l,\pm m}}, \quad (34)$$

and, ignoring the difference in the coefficients at  $H_l^m$ , we get

$$\frac{A_+}{A_-} = \sqrt{\frac{I_+}{I_-}}. \quad (35)$$

If this ratio is not too different from unity then, upon introducing

$$I \equiv \sqrt{I_- I_+}, \quad A_l^2 \equiv 2A_+ A_-, \quad (36)$$

we reduce equations describing such interaction to Eqs. (17), (18), and (21) which describe the two-mode resonance.

## 4 Stationary Solutions

Stationary, or fixed-point solutions of the amplitude equations are obtained from Eqs. (17), (18), and (21) where we set  $dA_j/d\tau = 0$ . Then the nonlinear frequencies are given by  $\omega_j + d\phi_j/d\tau$ , and, like the amplitudes, are constant.

### 4.1 Single-Mode Solutions

Eqs. (17), (18) admit single mode solutions

$$(A_0^0)^2 = \frac{1}{\alpha}, \quad (A_l^0)^2 = 0, \quad (37)$$

and

$$(A_0)^2 = 0, \quad (A_l)^2 = \frac{1-\gamma}{2\alpha H_l}. \quad (38)$$

It is of some interest to investigate stability of these solutions in the absence of resonances. Perturbation of Eqs. (17) and (18) with  $R \equiv 0$  leads to a simple eigenvalue problem for the growth rate  $\beta$ . We find for the radial mode solution  $\beta = -2$  and  $-(1+\gamma)$ . Thus, this is a stable solution. For the nonradial mode solution we find  $\beta = -1 - 3\gamma$  and  $1 - (1-\gamma)/H_l$ . The latter eigenvalue is less than zero, if  $\gamma < 1 - H_l$ . Since  $\gamma > 0$ , this may happen only for  $l=1$  because as we may see in Table 1  $H_l > 1$  for  $l > 1$ . This means that in principle we could expect that some of RR Lyr stars are  $l=1$  pulsators. However, we find it unlikely because even if  $\gamma$  is very small the growth of the  $l=1$  mode is much slower than that of  $l=0$ .

A survey of stability of radial pulsation to excitation of resonant nonradial modes in RR Lyr star models was given by DC. However, there was a need to repeat the calculations because of an error in the adopted form of the stability criterion. The correct criterion derived by VDK is

$$\Delta\omega^2 > |R_l^1|^2 (A_0^0)^2 - g^2 \quad (39)$$

where

$$g = \kappa_l + \Re(S_l^0) (A_0^0)^2 \quad (40)$$

is the nonlinear growth rate of the nonradial mode, and other symbols are the same as in Eq. (9). In our dimensionless notation Eq. (39) has the form

$$\Delta\sigma^2 > I^2 \left[ \frac{R^2}{\alpha^2} - (1+\gamma)^2 \right], \quad (41)$$

where we used Eq. (37) and the nonlinear growth rate of the nonradial mode is easily obtained from Eq. (18). In statistical approach, the above criterion implies that the probability of instability of radial-mode fixed-point solution is given by

$$P_l = \frac{I\sqrt{R^2/\alpha^2 - (1+\gamma)^2}}{\Delta\sigma_{\max}} \quad (42)$$

where  $\Delta\sigma_{\max}$  is the maximum absolute value of the detuning parameter, which in the case of dense spectra of nonradial modes in RR Lyr stars is given by a half of the frequency distance between consecutive nonradial modes,  $(\sigma_{l,n} - \sigma_{l,n+1})/2$ .

DC calculated probabilities of excitation of nonradial modes in the three sets of RR Lyr models. However, they used erroneously  $-I\gamma$  (in our notation) as the nonlinear damping rate of the nonradial mode. From our AEs we get the damping rate  $-I(1+\gamma)$ , which implies lower probabilities of excitation of nonradial modes, in particular in those cases where  $\gamma$  is very small and  $\alpha$  is comparable to  $R$ . This is what happens in the first overtone vicinity.

We calculated these probabilities once again for the DC RR Lyr models using the  $R, \gamma, I, \Delta\sigma_{\max}$  parameters inferred from the data given in DC. We adopted  $\alpha=200$  for the fundamental mode pulsation and 1200 for the first overtone,

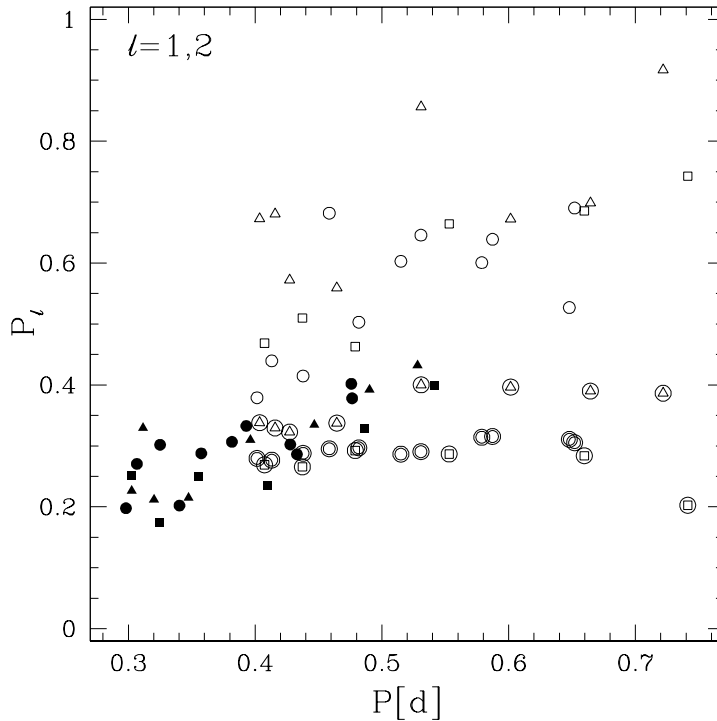


Fig. 1. Probabilities of excitation of nonradial modes with  $l=1,2$  in the models of DC. Solid and empty symbols denote modes in first overtone and in vicinity of fundamental mode, respectively. Encircled symbols indicate  $l=2$  (only for fundamental mode vicinity). Symbols are the same as in DC and refer to evolutionary tracks of different initial parameters. Squares and circles denote models characterized by ZAHB composition  $Z=0.001$ ,  $Y_{\text{HB}}=0.243$  and masses  $0.65$  and  $0.67 M_{\odot}$ , respectively. These quantities for models denoted by triangles are  $Z=0.0002$ ,  $Y_{\text{HB}}=0.24$  and  $0.74 M_{\odot}$ .

which, according to Eq. (37), correspond to  $A_0^0=0.0707$  and  $A_0^0=0.0289$ , respectively. These values may be regarded typical for RRab and RRc stars, respectively, and we will use them for all numerical calculations in this paper. Our calculations confirm DC's result that the most probably unstable are the  $l=1,5,6$  modes in the fundamental mode vicinity and the  $l=1,4$  modes in the first overtone vicinity. However, in the former vicinity we now find relatively higher probability of excitation for the  $l=2$  modes. The probabilities are presented in Figs. 1 and 2.

## 4.2 Double-Mode Solutions

When all amplitudes are constant and non-zero, we also have constant  $\Gamma$ , as can be seen in Eqs. (17), (18), and (21) or in Eqs. (25)–(27) and (31). Constant  $\Gamma$  implies the nonlinear frequencies to fulfill exactly the resonance condition, *i.e.*, phase-lock phenomenon. For the 1:1 resonance it means the equality of

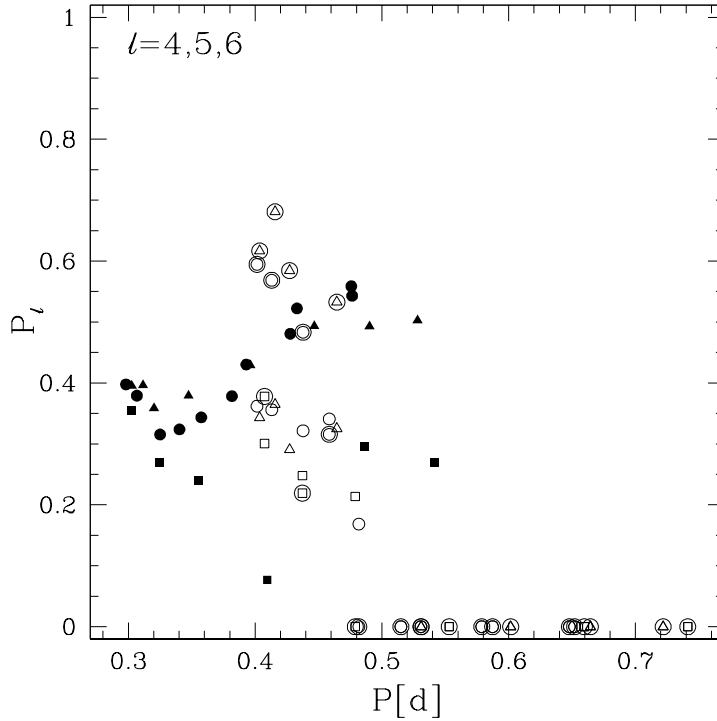


Fig. 2. The same as in Fig. 1, but for the modes with  $l=4$  (overtone),  $l=5$  (fundamental) and  $l=6$  (fundamental, encircled).

the two frequencies, while for the 2:1+1 resonance it means that the three frequencies are equidistant with the radial mode frequency being in the center of the triplet (see. Eqs. 12 and 23, respectively). Buchler *et al.* (1997) give general discussion of the phase-lock for other resonances.

Using Eqs. (17), (18), and (21) we can express the amplitudes and the detuning parameter in terms of the relative phase as follows

$$(A_0^{\text{dm}})^2 = \frac{R \sin \Gamma_{\text{dm}} (1 - \gamma) - 2\alpha (H_l - 1 + \gamma)}{2\alpha^2 (2 - H_l) - (R \sin \Gamma_{\text{dm}})^2}, \quad (43)$$

$$(A_l^{\text{dm}})^2 = \frac{\alpha (1 + \gamma) - R \sin \Gamma_{\text{dm}}}{2\alpha^2 (2 - H_l) - (R \sin \Gamma_{\text{dm}})^2}, \quad (44)$$

$$\Delta\sigma = R \cos \Gamma_{\text{dm}} [(A_l^{\text{dm}})^2 - I (A_0^{\text{dm}})^2]. \quad (45)$$

In general it is impossible to obtain an explicit expression for  $\Gamma_{\text{dm}}$  as a function of  $\Delta\sigma$ . Thus, fixed-point solutions have to be studied numerically. However, one important property of the solutions can be obtained analytically. Let us consider transition between single- and double-mode fixed-point, *i.e.*, the vicinity of  $A_l^{\text{dm}} = 0$ . Then  $R \sin \Gamma = \alpha (1 + \gamma)$  and  $A_0^{\text{dm}} = A_0^0$  (see Eqs. 43, 44, and 37).

With the help of these expressions we get from Eq. (45)

$$|\Delta\sigma| = \Delta\sigma_d \equiv \frac{IR}{\alpha} \sqrt{1 - \frac{\alpha^2}{R^2}(1+\gamma)^2} = I \sqrt{\frac{R^2}{\alpha^2} - (1+\gamma)^2}. \quad (46)$$

Note that it is the same critical value of  $\Delta\sigma$  as given by Eq. (41). It means that the nonradial mode appears with zero amplitude at the onset of instability. Further, it may be shown analytically that for  $|\Delta\sigma| > \Delta\sigma_d$  there are no double-mode solutions for which  $A_l/A_0 \ll 1$ . The analysis is not reproduced here but the property will be seen in our numerical examples.

The value of  $\Delta\sigma_d$  is critical for the consequences of the resonances considered here. For  $|\Delta\sigma| > \Delta\sigma_d$  the single-mode fixed-point solution is stable. For  $|\Delta\sigma| < \Delta\sigma_d$  it is unstable, but a double-mode fixed-point occurs. It will be shown that this double-mode fixed-point solution is almost always stable.

### 4.3 Stability of Double-Mode Fixed-Point Solution

Let us note that Eqs. (17), (18), (21) can be presented in the form

$$\frac{dA_0^2}{d\tau} = 2(1 - \alpha A_0^2 - 2\alpha A_l^2 - R \sin \Gamma A_l^2) A_0^2, \quad (47)$$

$$\frac{dA_l^2}{d\tau} = 2I(1 - \gamma - 2\alpha A_0^2 - 2H_l \alpha A_l^2 + R \sin \Gamma A_0^2) A_l^2, \quad (48)$$

$$\frac{d \sin \Gamma}{d\tau} = 2 \cos \Gamma [\Delta\sigma + R \cos \Gamma (IA_0^2 - A_l^2)]. \quad (49)$$

Let us now consider a small perturbation of the double-mode fixed-point solution,

$$A_0^2 = (A_0^{\text{dm}})^2 + \delta A_0^2, \quad A_l^2 = (A_l^{\text{dm}})^2 + \delta A_l^2, \quad (50)$$

$$\sin \Gamma = \sin \Gamma_{\text{dm}} + \delta \sin \Gamma, \quad \cos \Gamma = \cos \Gamma_{\text{dm}} + \delta \cos \Gamma. \quad (51)$$

Now we insert the above quantities to Eqs. (47)–(49) and neglect terms of second and higher orders with respect to small perturbations. In this way we obtain a system of linear differential equations which can be written in a matrix form

$$\frac{d\mathbf{X}}{d\tau} = \mathbf{A}\mathbf{X} \quad (52)$$

where

$$\mathbf{X} = \begin{bmatrix} \delta A_0^2 \\ \delta A_l^2 \\ \delta \sin \Gamma \end{bmatrix} \quad (53)$$

and

$$\mathbf{A} = 2 \begin{bmatrix} -\alpha A_0^2 & -(2\alpha + R \sin \Gamma) A_0^2 & -R A_0^2 A_l^2 \\ I(-2\alpha + R \sin \Gamma) A_l^2 & -2I H_l \alpha A_l^2 & I R A_0^2 A_l^2 \\ I R (1 - \sin^2 \Gamma) & -R (1 - \sin^2 \Gamma) & -R \sin \Gamma (I A_0^2 - A_l^2) \end{bmatrix}. \quad (54)$$

We made use of  $\cos^2 \Gamma = 1 - \sin^2 \Gamma$ ,  $\cos \Gamma \delta \cos \Gamma = -\sin \Gamma \delta \sin \Gamma$  relations and omitted sub- and superscripts  $dm$  denoting double-mode fixed-point solution.

Eq. (52) implies time dependence of the perturbations in the exponential form,  $\exp(\lambda\tau)$ . There are three eigenvalues determined by the following cubic equation

$$\lambda^3 + a_1\lambda^2 + a_2\lambda + a_3 = 0 \quad (55)$$

where

$$a_1 = \alpha(A_0^2 + 2IH_l A_l^2) + R \sin \Gamma (IA_0^2 - A_l^2), \quad (56)$$

$$a_2 = I\alpha^2 A_0^2 A_l^2 (2H_l - 4) + \alpha R \sin \Gamma (IA_0^2 - A_l^2) (A_0^2 + 2IH_l A_l^2) + IR^2 A_0^2 A_l^2 (2 - \sin^2 \Gamma), \quad (57)$$

$$a_3 = IA_0^2 A_l^2 [R \sin \Gamma (IA_0^2 - A_l^2) (R^2 - \alpha^2 (4 - 2H_l)) + R^2 (1 - \sin^2 \Gamma) \alpha (A_0^2 (1 + 2I) + 2A_l^2 (1 + IH_l))]. \quad (58)$$

The stationary solution is stable when all three eigenvalues have negative real parts. The condition for the stability is then given by Hurwitz criteria

$$a_1 > 0, \quad (59)$$

$$a_1 a_2 - a_3 > 0, \quad (60)$$

$$a_3 > 0. \quad (61)$$

We will check these inequalities numerically to determine stability of each of our stationary solutions.

#### 4.4 Numerical Examples

In this Section we will show examples of double-mode fixed-point solutions for the models from DC and will discuss their stability. The solution is characterized by the parameters  $\gamma$ ,  $R$ ,  $\alpha$ ,  $I$ ,  $\Delta\sigma$ . For the detuning parameter  $\Delta\sigma$  we will consider the range of values from 0 to  $\Delta\sigma_{\max}$ .

We choose representative examples of nonradial modes which have the highest excitation probability in the vicinity of the fundamental mode and the first overtone.

In Figs. 3–5 we plot  $A_0, A_l$ , and  $\sin \Gamma$  as functions of  $\Delta\sigma$ . As one can see there are at least two branches of stable solutions in most cases. In the figures the branches are marked with  $a$  and  $b$ . The third branch that is present in some cases is always unstable and we will not be interested in it. The  $a$ -branch exists for  $\Delta\sigma < \Delta\sigma_d$ , *i.e.*, in the region where the single-mode fixed-point is unstable, as discussed in Sections 4.1 and 4.2. This branch is stable except for a very small region near  $\Delta\sigma = 0$  in the case of the  $l = 1$  mode at the first overtone (Fig. 5, left panels). We are not sure whether this instability is real or rather an artifact of our simplifications.

The conclusion is that there exists one or two stable stationary solutions for all possible values of  $\Delta\sigma$  because in the region where  $a$ -branch does not exist, the single-mode fixed-point is stable. Which one of these solutions, if any, is

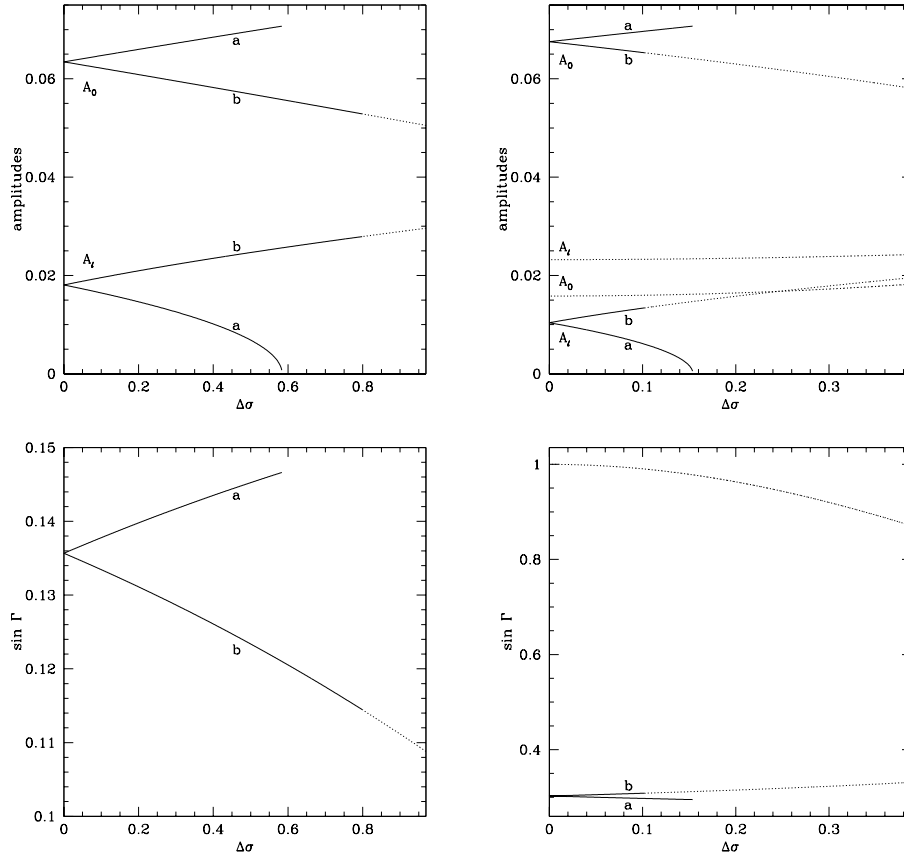


Fig. 3. Fixed-point solutions for the resonance between the fundamental mode and the nonradial modes with  $l=1$  (left panels) and  $l=2$  (right panels). The  $\Delta\sigma$ -dependence of amplitudes (upper panels) and  $\sin\Gamma$  (lower panels) are shown. Solid and dotted lines denote stable and unstable solutions, respectively. The range of  $\Delta\sigma$  corresponds to  $\Delta\sigma_{\max}$ , *i.e.*, to the density of the spectra of nonradial modes. The adopted coefficients are  $R=1456$ ,  $\gamma=0.068$ ,  $I=0.0811$  for  $l=1$  and  $R=1362$ ,  $\gamma=1.0099$ ,  $I=0.0237$  for  $l=2$ .

chosen by the system will be studied by numerical integration of the amplitude equations.

## 5 Time Dependent Solutions

In this Section we present time dependent solutions obtained by means of numerical integration of AEs for the same values of coefficients that were used in the stationary solution studies. We focus on the  $l=1$  cases but the results are similar in other cases.



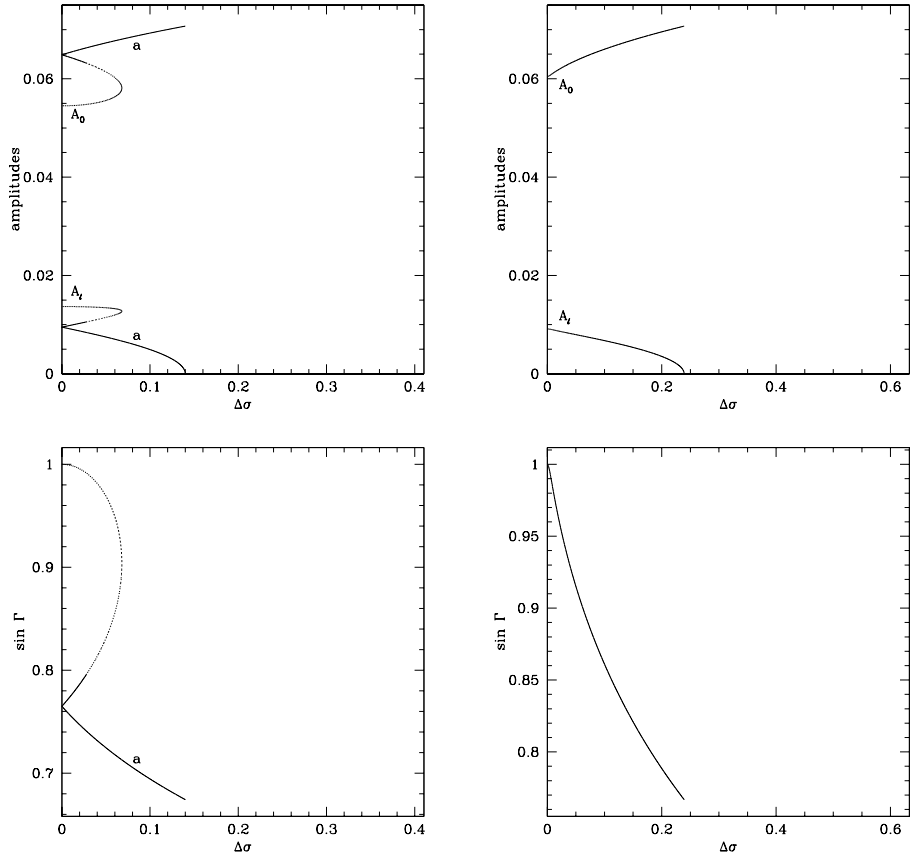


Fig. 4. The same as in Fig. 3 but for the nonradial modes with  $l=5$  (left panels) and  $l=6$  (right panels). The adopted coefficients are  $R=1771$ ,  $\gamma=4.9738$ ,  $I=0.0214$  for  $l=5$  and  $R=2814$ ,  $\gamma=9.7903$ ,  $I=0.0265$  for  $l=6$ .

## 5.1 Examples

Figs. 6 and 7 show the solutions for the resonance between the fundamental and  $l=1$  modes for the selected values of the detuning parameter and different initial parameters. In Fig. 6 the detuning parameter of 0.3 is in the range where the  $a$ -branch exists. The two stationary solutions are  $A_0^a \approx 0.067$ ,  $A_l^a \approx 0.013$ ,  $\sin \Gamma_a \approx 0.142$  and  $A_0^b \approx 0.059$ ,  $A_l^b \approx 0.022$ ,  $\sin \Gamma_b \approx 0.129$  (see Fig. 3, left panels). Both solutions are stable. In the left panels we show the development of the instability beginning with very small pulsation amplitudes. The final (asymptotic) state is an  $a$ -branch solution. In the right panels the initial conditions are close to a  $b$ -branch solution which is another asymptotic state of the system.

In Fig. 7 the detuning parameter is 0.65 and, as can be seen from Fig. 3, left panels, it is in the range where the  $a$ -branch does not exist. Instead we have stable single-mode solution  $A_0^0=0.0707$ ,  $A_l^0=0$ . The second stable solution is

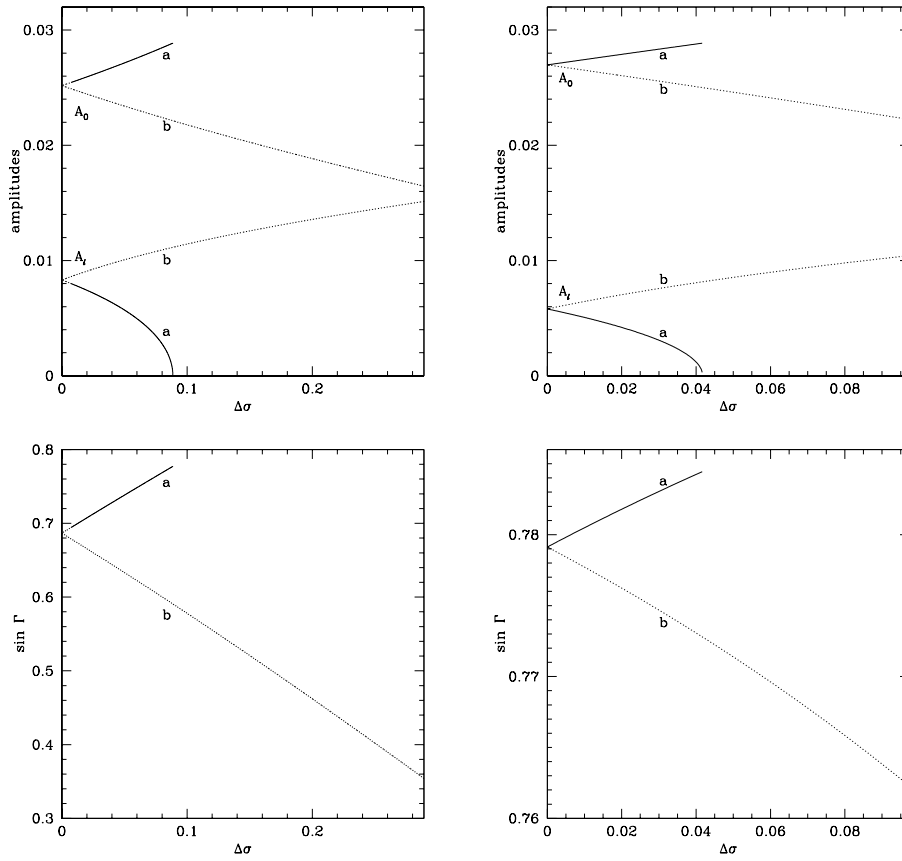


Fig. 5. The same as in Figs. 3 and 4 but for the first overtone and the nonradial modes with  $l=1$  (left panels) and  $l=4$  (right panels). The following values of the coefficients were adopted:  $R=1550$ ,  $\gamma=0.044$ ,  $I=0.1090$  for  $l=1$  and  $R=1748$ ,  $\gamma=0.1427$ ,  $I=0.0462$  for  $l=4$ .

the  $b$ -branch solution  $A_0^b \approx 0.055$ ,  $A_l^b \approx 0.026$ ,  $\sin \Gamma_b = 0.119$ . The initial conditions in the left panels are very close to the  $b$ -branch solution and this solution is the asymptotic state. In the right panels we start only slightly farther from the  $b$ -branch than in the left panels, but the asymptotic state is completely different, *i.e.*, it is the single-mode solution.

As we discussed in Section 4.4 there might be a very narrow range around  $\Delta\sigma=0$  where  $a$ -branch solutions are unstable. We found numerically an amplitude modulated solution with the period of about 60 in dimensionless units. The range is very narrow and we do not know how robust this finding is. In other cases, the asymptotic state is always a stationary solution. Hence we focus here only on fixed-point asymptotic solutions.

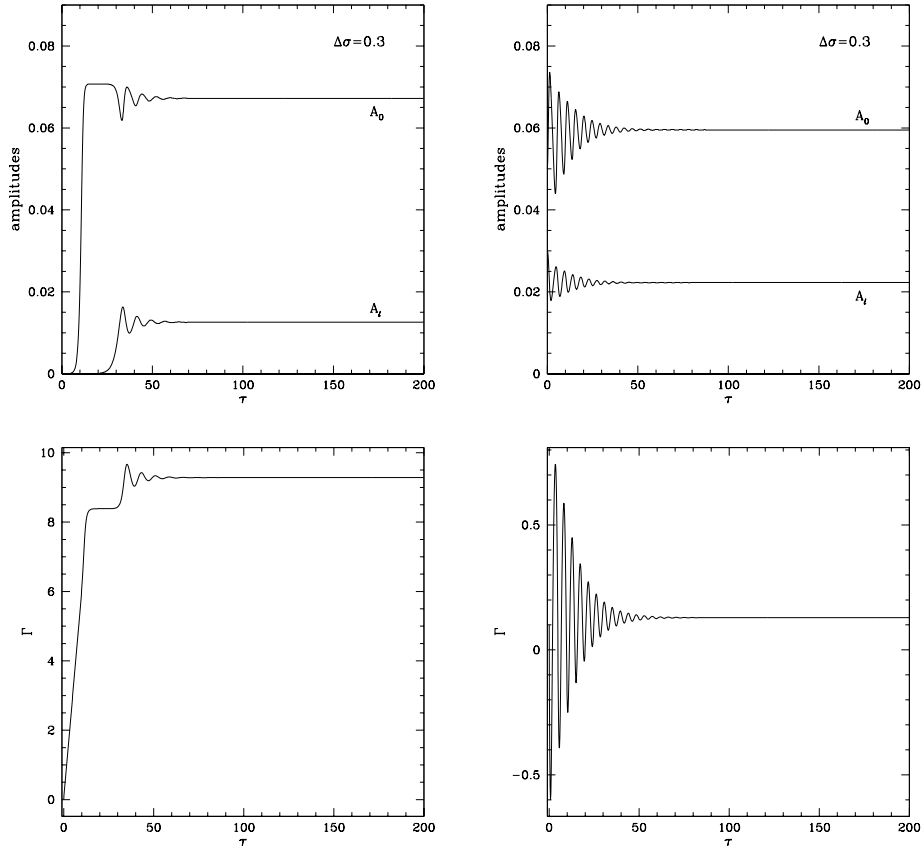


Fig. 6. Time dependent solutions for the same coefficients as used in the left panels of Fig. 3, and the detuning parameter 0.3. The initial parameters are  $A_0 = A_l = 0.00001$ ,  $\Gamma = 0$  (left panels) and  $A_0 = 0.05$ ,  $A_l = 0.03$ ,  $\Gamma = 0.1$  (right panels).

## 5.2 Regions of Attraction for the Asymptotic Solutions

Here we present results of a more systematic survey of the time dependent solutions. We determine the ranges of the initial conditions (regions of attraction) leading to different asymptotic solutions.

Fig. 8 shows the regions of attraction for the resonance between the fundamental radial mode and the nonradial  $l=1$  mode. The stationary solutions for the adopted coefficients are shown in the left panels of Fig. 3. Fig. 9 shows the same solutions in the case of the resonance between the fundamental radial mode and the nonradial  $l=2$  mode. The stationary solutions for the corresponding cases are shown in the right panels of Fig. 3.

We made similar computations for other values of  $\Delta\sigma$  and other pairs of modes. We found the following properties of the attraction regions. Except for the small region near the center of resonance in the case of the first overtone

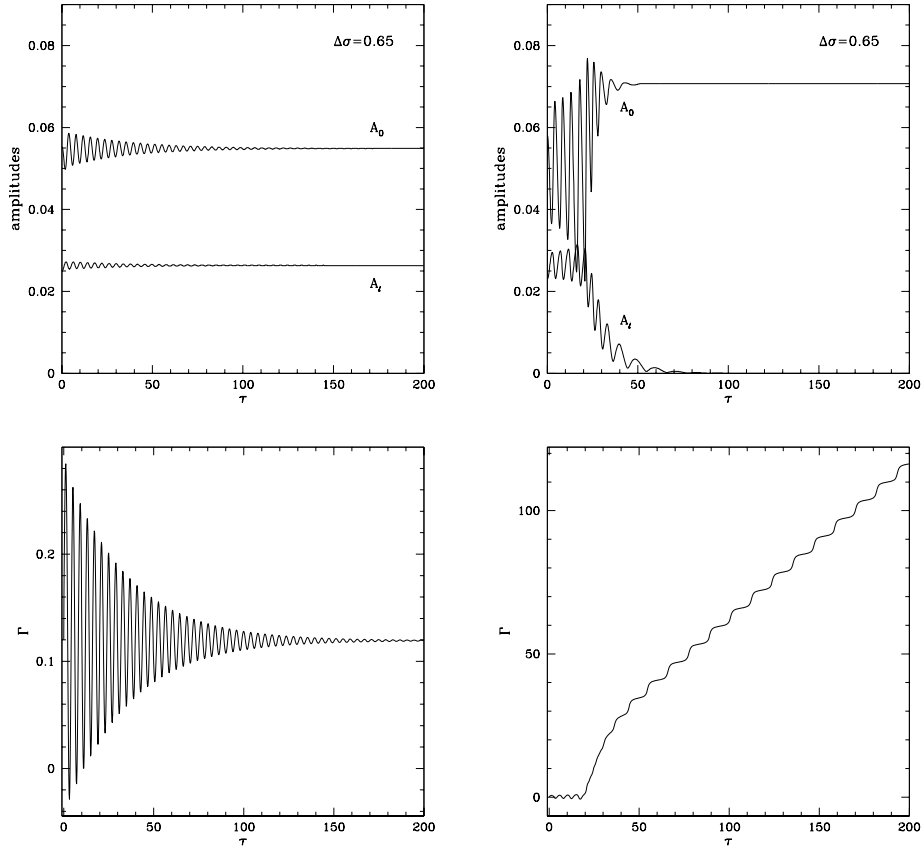


Fig. 7. Time dependent solutions for the same coefficients as used in the left panels of Fig. 3, and the detuning parameter 0.65. The initial parameters are  $A_0 = 0.055$ ,  $A_l = 0.025$ ,  $\Gamma = 0.12$  (left panels) and  $A_0 = 0.058$ ,  $A_l = 0.023$ ,  $\Gamma = 0.1$  (right panels).

and  $l=1$  mode, that was discussed in Sections 4.4 and 5.1, all the attractors are fixed-point solutions. When  $b$ -branch solutions are stable they can be attractors simultaneously with  $a$ -branch or single-mode stationary solutions. When  $b$ -branch solutions are unstable then the only asymptotic states are  $a$ -branch solutions if  $\Delta\sigma < \Delta\sigma_d$  or single-mode solutions if  $\Delta\sigma > \Delta\sigma_d$ .

From inspection of Figs. 8 and 9 we may conclude that the higher are the values of  $A_l$  the smaller are the regions of attraction to the  $b$ -branch. In other words, the farther is the  $b$ -branch from the lower ( $a$ -branch or single mode) stationary solution, the lower is the probability of finding the  $b$ -branch pulsation. In the three dimensional space of the initial parameters the regions of attraction to the  $b$ -branch are significantly smaller than those to the  $a$ -branch or the single mode solution. Let us note also that the star entering the instability strip may begin its pulsation only as a single mode pulsator or an  $a$ -branch pulsator. Except for the exact resonance, a phase transition to a  $b$ -branch pulsation requires a finite energy input. Consequently, we will ignore  $b$ -branch solutions in the

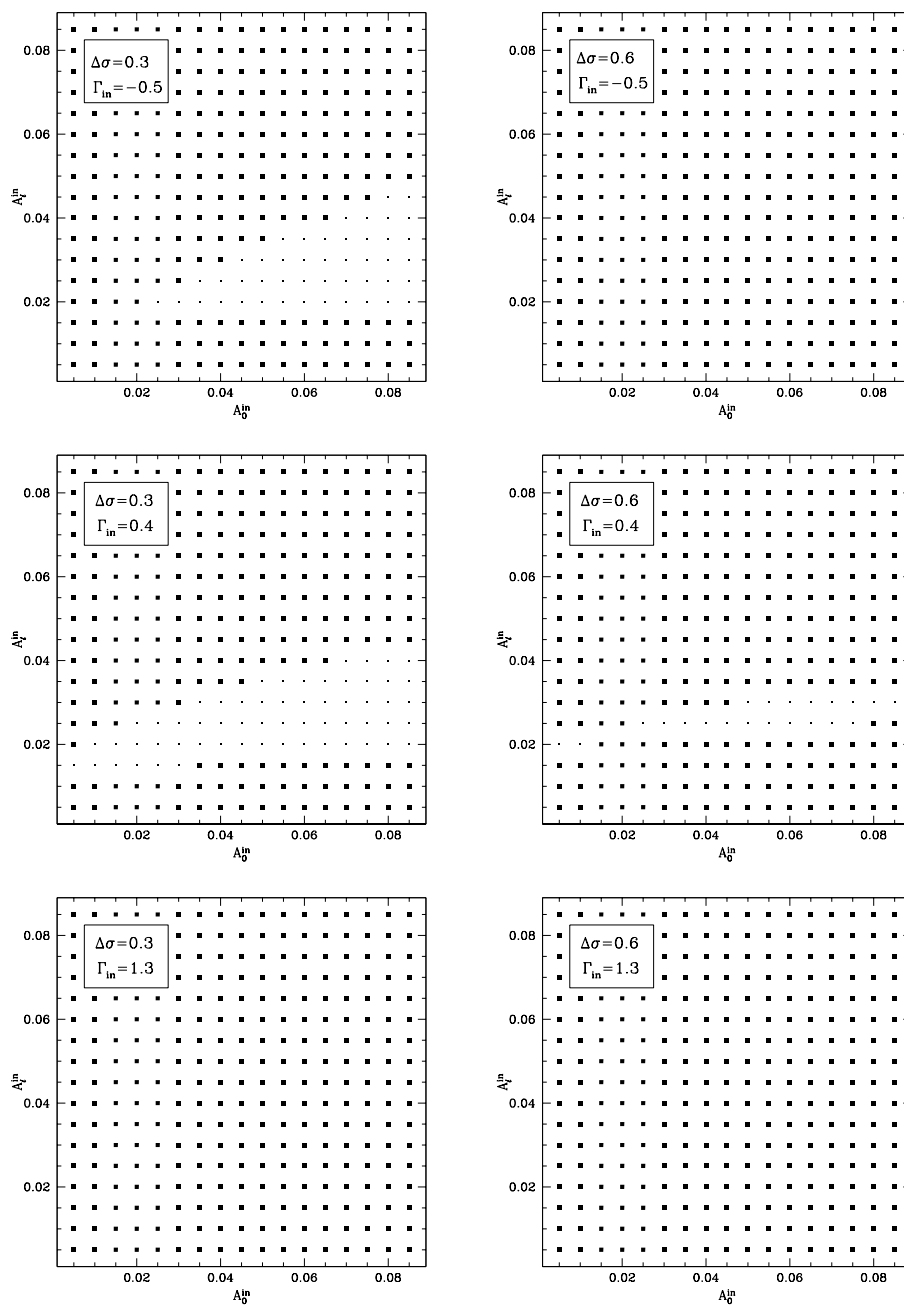


Fig. 8. Regions of attraction for asymptotic solutions for the resonance between the fundamental and the  $l=1$  modes (see Fig. 3, left panels). Squares denote attraction to the  $a$ -branch ( $\Delta\sigma=0.3$ ) or to the single-mode fixed-point ( $\Delta\sigma=0.6$ ) solution. Dots denote attraction to the  $b$ -branch.

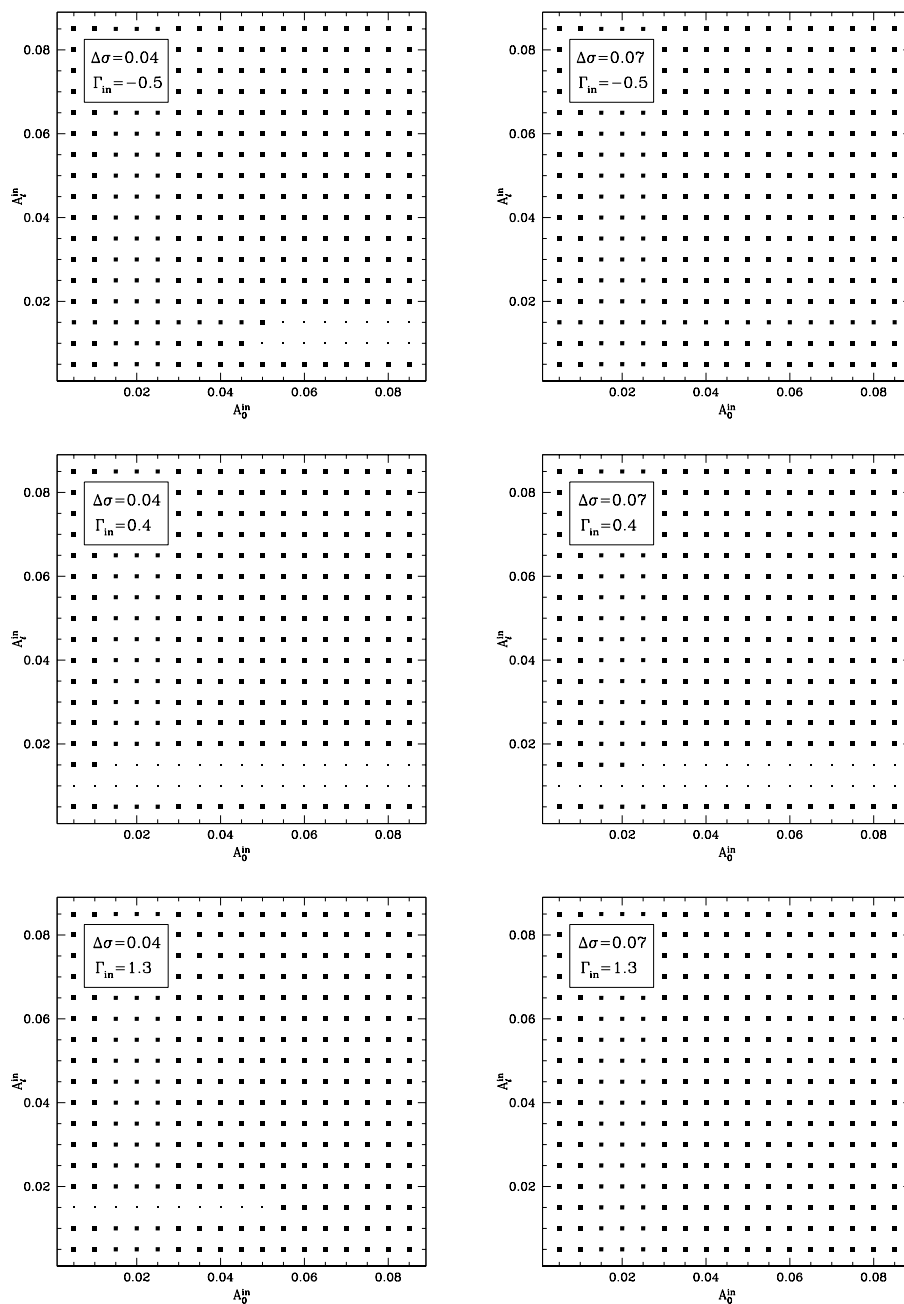


Fig. 9. Regions of attraction for asymptotic solutions for the resonance between the fundamental and the  $l=2$  modes (see Fig. 3, right panels). Squares and dots denote attraction to the  $a$ - and  $b$ -branch, respectively.

foregoing considerations.

We see in Figs. 3–5 that if  $b$ -branch solutions are ignored the maximum values of the  $A_l/A_0$  ratio is at  $\Delta\sigma=0$ . Thus, we may conclude that the strongest influence of the resonant nonradial mode excitation on pulsation is at the exact resonance. From now on we focus on this special case.

## 6 The Role of Nonradial Modes in Constant Amplitude Pulsation

In this Section we calculate reduction of the radial mode amplitude,  $A_0/A_0^0$ , and the relative period change,  $\Delta P/P$ , caused by the resonant nonradial mode excitation. We also calculate the relative amplitude of the nonradial mode,  $A_l/A_0$ , whose presence may perhaps be detected by means of spectroscopy.

### 6.1 Analytical Expressions

As we explained above we assume  $\Delta\sigma=0$ . Then, if  $\cos\Gamma \neq 0$ , from Eq. (45) we immediately get

$$(A_l^s)^2 = I(A_0^s)^2, \quad (62)$$

or

$$\frac{A_l^s}{A_0^s} = \sqrt{I}. \quad (63)$$

If  $\cos\Gamma=0$  then we are not in the  $a$ -branch for most of the cases considered. The exception is the case in which there is no  $b$ -branch. The example is seen in the right panels of Fig. 4. In such a situation the amplitude ratio is determined by Eqs.(43) and (44) where we set  $\sin\Gamma=1$ . It happens only in a few cases in our large set of resonant mode pairs and we do not consider it in detail. It is sufficient to note that the true value of  $A_l/A_0$  is always a bit smaller than  $\sqrt{I}$  which we adopt in our calculation.

In the case of two nonaxisymmetric modes the amplitude of the  $m=\pm 1$  modes is given by  $A_{\pm} = A_l/\sqrt{2}$ , which implies

$$\frac{A_{\pm}^s}{A_0^s} = \sqrt{\frac{I}{2}}. \quad (64)$$

From Eqs. (43), (44) and Eq. (62) we obtain

$$R\sin\Gamma_s = \alpha \frac{1 + \gamma + 2I(H_l - 1 + \gamma)}{1 + I(1 - \gamma)}. \quad (65)$$

When  $\sin\Gamma_s$  obtained with the above expression is bigger than 1 we should use  $\sin\Gamma_s=1$ . This is the case of the absence of the  $b$ -branch discussed above. We will not show any numerical results for this case.

After inserting solution given by Eq. (65) into Eq. (43) we obtain

$$(A_0^s)^2 = \frac{1}{\alpha} \cdot \frac{1 + I(1 - \gamma)}{1 + 2I(2 + IH_l)}, \quad (66)$$

which implies

$$\frac{A_0^s}{A_0^0} = \sqrt{\frac{1 + I(1 - \gamma)}{1 + 2I(2 + IH_l)}}. \quad (67)$$

For the relative change of the radial mode period caused by nonradial mode excitation we get using Eq. (19),

$$\frac{|\Delta P_s|}{P} = \frac{|\delta\sigma_s|}{\sigma_0} = \frac{R}{\sigma_0} |\cos\Gamma_s| (A_l^s)^2. \quad (68)$$

The sign of  $\cos\Gamma_s$  is undetermined at  $\Delta\sigma = 0$ . In the rest of the  $a$ -branch the sign of  $\cos\Gamma$  is opposite to the sign of  $\Delta\sigma$ . Thus, the frequency shift can be either positive or negative with equal probabilities. From Eq. (65) we obtain

$$|R\cos\Gamma_s| = \sqrt{\frac{R^2 - \alpha^2 (1 + \gamma + 2I(H_l - 1 + \gamma))^2}{(1 + I(1 - \gamma))^2}}. \quad (69)$$

For the dimensionless frequency we use

$$\sigma_0 = \frac{\omega_0}{\kappa_0} = \frac{2\pi}{P\kappa_0}. \quad (70)$$

Finally, with the help of Eqs. (62), (66), (69), (70) we get from Eq. (68)

$$\begin{aligned} \frac{|\Delta P_s|}{P} &= \frac{P\kappa_0}{2\pi} \cdot \frac{I}{1 + 2I(1 + 2IH_l)} \times \\ &\times \sqrt{\frac{R^2}{\alpha^2} (1 + I(1 - \gamma))^2 - (1 + \gamma + 2I(H_l - 1 + \gamma))^2}. \end{aligned} \quad (71)$$

In a few cases of the lack of the  $b$ -branch the period change is exactly zero. Eqs. (67) and (71) allow us to evaluate the relative change of the amplitude and period, respectively, for the radial mode caused by a resonant excitation of nonradial mode. In the right-hand side we have quantities that may be calculated for specified model and mode. The nonradial mode amplitude can be calculated with Eq. (63).

## 6.2 Application to Evolutionary Models of RR Lyr Stars

We apply here the formulae of the previous Section to our models of RR Lyr stars. Like in Section 4.1 we considered the resonance between the radial and the nearest nonradial modes of  $l = 1, 2, 5, 6$ , for fundamental mode, and of  $l = 1, 4$ , for first overtone. Using the same mode parameters we calculated the nonradial



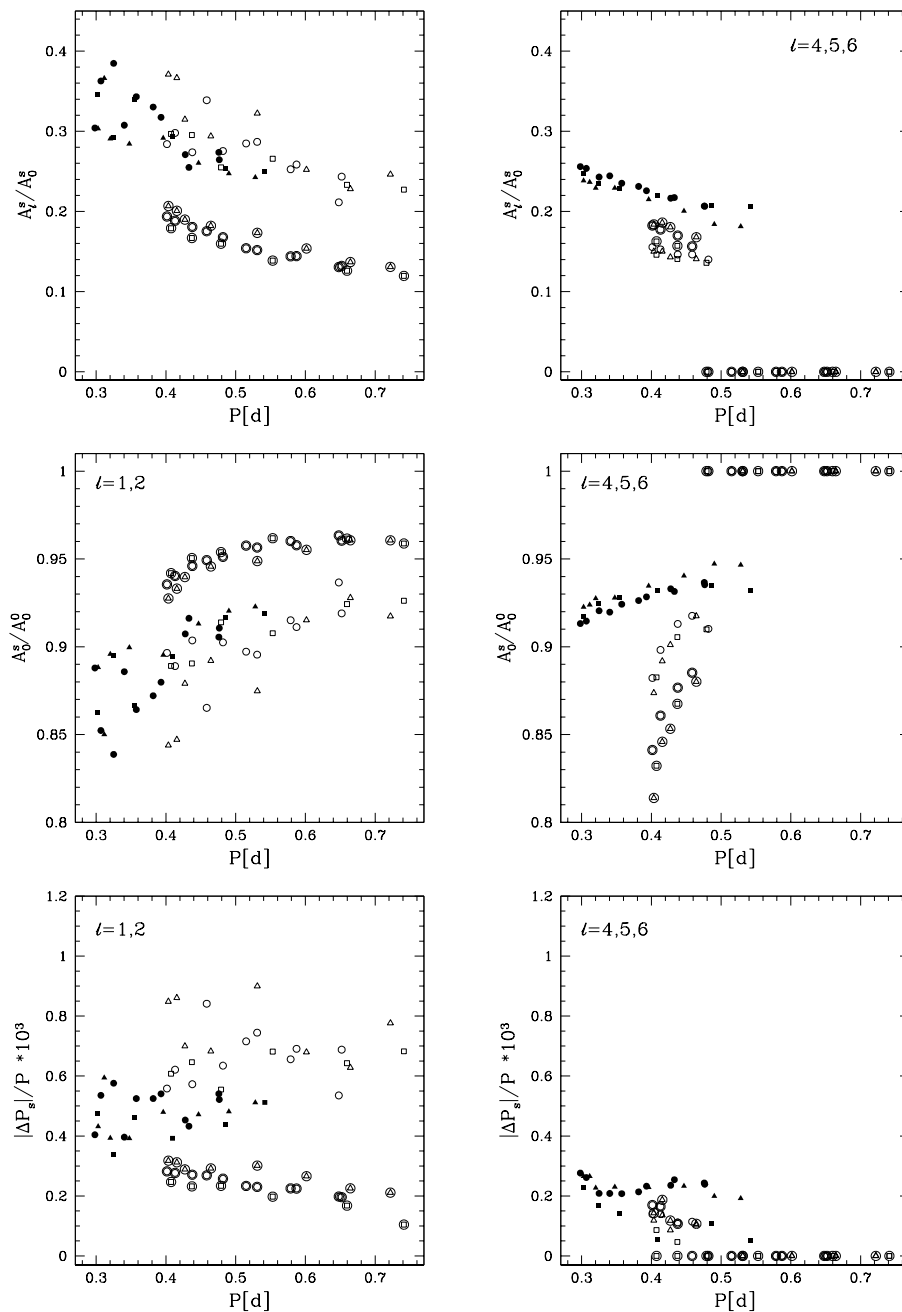


Fig. 10. Finite amplitude consequences of the 1:1 resonance between the radial and the selected nonradial modes. Different symbols correspond to different RR Lyr models and different modes (see Fig. 1 for more detailed explanation). The top panels show the relative amplitudes of the nonradial modes. The middle panels show the ratio of the resonant to the nonresonant radial mode amplitudes. The bottom panels show the relative period shift due to the resonance.

mode amplitudes, Eq. (63), the reduced radial mode amplitudes, Eq. (67) and the relative period changes, Eq. (71). Results are given in Fig. 10. The values give the maximum effect of the resonance because – we recall –  $\Delta\sigma = 0$  was assumed.

We see in the top panels that the nonradial mode amplitude may be quite large. Still detecting the presence of nonradial modes, which would constitute an ultimate test for our theory, may not be easy. In the case of low degree nonradial modes, the determination of  $l$  by means of multicolor photometry is feasible (see *e.g.*, Garrido 2000). We should stress, however, that the technique has been applied so far only to main sequence pulsators and with only a moderate success. For higher degree modes ( $l > 2$ ) one may contemplate use of line profile variations (see *e.g.*, Aerts and Eyer 2000). Again in this case the technique has been used only for the main sequence pulsators.

The amplitude reduction caused by the resonance, which is shown in the middle panels, is significant in some cases. Note, in particular, in the right panel the relatively large reduction caused by higher degree modes. The implication is that the pulsation amplitude must be regarded as a random quantity in certain ranges. It is random because the detuning parameter  $\Delta\sigma$  which affects the amplitude is in fact a random quantity in the  $[0, \Delta\sigma_{\max}]$  range.

However, in the case of low-degree nonradial modes, the primary source of uncertainty of observable amplitude prediction is the orientation of the pulsation axis. We will now focus on  $l = 1$  mode and will convert amplitudes shown in Fig. 10 to those of light and radial velocity.

In Appendix B.1 we derive formulae for the radial velocity and light curve amplitudes. With the help of Eq.(B9) we get the ratio of radial velocity amplitude with the presence of the nonradial mode,  $A_v$ , to that without the nonradial mode,  $A_{v,0}$ . The expression is

$$\frac{A_v}{A_{v,0}} = \sqrt{1 + \epsilon_v^2 + 2\epsilon_v \cos(\Gamma/2)} \quad (72)$$

where for  $l = 1$  we have

$$\epsilon_v = 1.35 A_1/A_0 \cos \Theta_0. \quad (73)$$

Here  $\Theta_0$  is the aspect angle,  $A_1/A_0$  is the calculated amplitude ratio, whose maximum values are shown in the top panels of Fig. 10.

Similarly, we get for the light amplitude ratio

$$\frac{A_{M\text{bol}}}{A_{M\text{bol},0}} = \sqrt{1 + \frac{\epsilon_M^2}{p_0^2} + \frac{2\epsilon_M}{p_0^2} \left[ \frac{2}{f} \cos(\psi + \Gamma/2) + \cos(\Gamma/2) \right]} \quad (74)$$

(see Eqs. B12, B19, and B21). For  $l = 1$

$$\epsilon_M = 1.23 A_1/A_0 \cos \Theta_0. \quad (75)$$

The complex quantity  $f e^{i\psi}$  is the ratio of the perturbed radiative flux to radial displacement at the surface. It is determined from linear nonadiabatic calculations. We also denoted

$$p_0 = \sqrt{1 + \frac{4}{f} \cos \psi + \frac{4}{f^2}}. \quad (76)$$

When we assume the maximum value of the  $A_1/A_0$  ratio to be about 0.3 the maximum absolute value of  $\epsilon$  is about 0.4 and 0.37 for the radial velocity and the light variations, respectively. The largest effect is for  $|\cos(\Gamma/2)| = 1$ . Note that for  $l=1$  modes we get  $\Gamma \approx 0$  or  $2\pi$ . Then the *rhs* in Eq. (72) is  $1 \pm \epsilon_v$ . Since  $\epsilon_v$  is a random quantity with values between  $-0.4$  and  $0.4$ , the range of the ratio  $A_v/A_{v,0}$  ranges from 0.6 to 1.4.

For the light curve we have to discuss possible values of  $f$  and  $\psi$ . In our linear RR Lyr pulsation models  $f$  ranges from about 2 to over 10. The phase  $\psi$  is correlated with  $f$  so that it is close to zero for  $f \approx 2$  and almost  $\pi/2$  for  $f > 10$ . For the lowest values of these quantities we have  $p_0 = 2$  (see Eq. 76) and  $A_{Mbol}/A_{Mbol,0} = \sqrt{1 + \epsilon_M^2/4 + \epsilon_M \cos(\Gamma/2)}$  (see Eq. 74). For  $|\cos(\Gamma/2)| = 1$  we obtain  $A_{Mbol}/A_{Mbol,0} = 1 \pm \epsilon_M/2$ . If  $f \gg 2$ , we easily obtain  $p_0 = 1$  and  $A_{Mbol}/A_{Mbol,0} = 1 \pm \epsilon_M$ , that is almost as wide range as in the case of the radial velocity amplitudes.

At higher  $l$ 's, the expected amplitude scatter should be much lower due to both the smaller  $A_l/A_0$  ratio and the effect of averaging over the stellar disc.

We conclude that certain scatter in the dependence of the pulsation amplitudes on stellar parameters should be expected. Let us note that the existence of such a dependence underlines empirical methods of absolute magnitude and metallicity determination employing light curve data (*e.g.*, Kovács and Jurcsik 1996, Jurcsik and Kovács 1996).

The period changes shown in the bottom panels of Fig. 10 are indeed rather small. Again they should be regarded as random quantities. The expected scatter is probably inconsequential for the empirical use of period data on RR Lyr stars.

## 7 Amplitude and Phase Modulation Due to Non-radial Mode Excitation

### 7.1 Theoretical Prediction

In Section 4.2 we showed that the stationary solution in the case of the 2:1+1 resonance is an equally-spaced triplet with the central peak corresponding to the radial mode and the two side-peaks corresponding to the nonradial modes. We will show here that excitation of the triplet manifests itself, in general, as pulsation with amplitude and phase modulation and thus provides a plausible explanation of the Blazhko effect. We focus on the  $l=1$  modes. Modes at  $l=2$  have significantly lower probability of excitation, as may be seen in Fig. 1, while those at  $l > 2$  have significantly lowered amplitudes due to the averaging effect, as discussed in Appendix B. We consider first an excitation of the  $m = \pm 1$  modes of the same radial order  $n$ .

In uniformly and slowly rotating stars the frequencies of the  $m = \pm 1$  modes are given by

$$\omega_{\pm} = \omega_0 \pm C\Omega + D\Omega^2, \quad (77)$$

where  $C$  (the Ledoux constant) and  $D$  depend on the stellar structure. In RR Lyr stars contribution to the Ledoux constant arises predominantly in the  $g$ -mode propagation zone and thus we can use the asymptotic value  $C = 1/2$  for  $l = 1$ . Values of  $D$  for  $l = 1$   $g$ -modes are very small. As first noted by Buchler *et al.* (1995), the resonant phase-lock effect changes the frequencies in such a way that  $D\Omega^2$  becomes zero. Eq. (77) yields frequencies in the corotating system. In the inertial system we have to add  $-m\Omega$ , which accounts for transformation of the azimuthal angle. Note that in our notation  $m = -1$  corresponds to prograde modes. Thus, for the nonradial mode frequencies in the inertial system we have the following relation

$$\omega_{\pm} = \omega_0 \mp \lambda \quad (78)$$

where  $\lambda = \Omega/2$ . Eq. (78) remains valid in the case of depth-dependent rotation, but then  $\Omega$  should be understood as the average rotational frequency weighted with the Brunt-Väisälä frequency, which is strongly peaked in the innermost part of the radiative interior.

In Appendix B.2 we show that when the amplitudes of  $l = 1$ ,  $m = \pm 1$  modes are equal and small in comparison with that of the radial mode, the radial velocity is given by

$$V_r = A_{v,0} [1 + a \cos \lambda t] \cos(\omega t - \pi/2 + b \cos \lambda t) \quad (79)$$

(see Eq. B24 and B36), where

$$a = \epsilon_v \cos(\Gamma/2), \quad (80)$$

$$b = \epsilon_v \sin(\Gamma/2). \quad (81)$$

The quantity  $\epsilon_v$  is defined similarly as in Eq. (73) but with  $\sin \Theta_0$  instead of  $\cos \Theta_0$ ,  $A_{v,0}$  is given in Eq. (B6). The maximum value of  $\epsilon_v$  is about 0.4. The largest amplitude modulation, factor of 7/3, is obtained for  $|\cos(\Gamma/2)| = 1$  and then there is no phase modulation. The opposite case of maximum phase modulation and no amplitude modulation corresponds to  $\cos(\Gamma/2) = 0$ . It is of interest that for  $l = 1$  we should be close to one of these two extreme cases, since we have  $\sin \Gamma \approx 0$ .

In a similar manner we obtained (see Appendix B.2 for details) the bolometric luminosity variations in the form

$$\Delta M_{\text{bol}} = A_{M_{\text{bol}},0} [1 + c \cos \lambda t] \cos(\omega t + \varphi_0 + d \cos \lambda t) \quad (82)$$

where

$$c = \frac{\epsilon_M}{p_0} \cos(\psi + \Gamma/2 - \varphi_0), \quad (83)$$

$$d = \frac{\epsilon_M}{p_0} \sin(\psi + \Gamma/2 - \varphi_0) \quad (84)$$

(see Eqs. B39, B47, and B48). Quantities  $p_0$  and  $\varphi_0$  are given by Eqs. (B13) and (B14). Explicit expression for  $p_0$  is also given by Eq. (76). For  $\epsilon_M$  we may

use *rhs* of Eq. (75) replacing  $\cos$  with  $\sin$ . The lowest values of  $f, \psi$  are close to 2 and 0, respectively. From Eqs. (B13)–(B14) we find  $p_0 \approx 2$ ,  $\varphi_0 \approx 0$ , which yields

$$c \approx \frac{\epsilon_M}{2} \cos(\Gamma/2), \quad (85)$$

$$d \approx \frac{\epsilon_M}{2} \sin(\Gamma/2). \quad (86)$$

For the highest values of  $f (\gg 2)$  we have  $\psi \approx \pi/2$  and we find  $p_0 \approx 1$ ,  $\varphi_0 \approx \pi/2$ , which yields

$$c \approx \epsilon_M \cos(\Gamma/2), \quad (87)$$

$$d \approx \epsilon_M \sin(\Gamma/2). \quad (88)$$

This means that we obtain the same conditions for pure amplitude and pure phase modulation as in the case of the radial velocity variation. Also the ranges of modulation are similar. However, at moderate values of  $f$  and  $\psi$  we may have significant both phase and amplitude modulations.

The 2:1+1 resonance may lead to excitation of certain modes from consecutive multiplets. The two distinct cases involve the following pairs of  $m$  values:  $(1, -1)$ ,  $(-1, 1)$ . The resonant interaction between a  $(0, 0)$  pair and the radial mode is also possible, but this case is described by much more complicated AEs and should be studied separately. Thus we focus here on the  $m = \pm 1$  pairs. Then the modulation frequency is

$$\lambda = \begin{cases} \frac{\Delta\omega - \Omega}{2} & \text{for } m's \quad (1, -1) \\ \frac{\Delta\omega + \Omega}{2} & \text{for } m's \quad (-1, 1) \end{cases} \quad (89)$$

where  $\Delta\omega$  is the frequency difference between centers of multiplets of the radial order  $n$  and  $n + 1$ . In this case we expect unequal amplitudes of the side-peaks in consequence of the inequality of mode inertia. In the  $(-1, 1)$  case the effect is systematic. It may be seen in Fig. 2 of DC that lower frequency modes have higher inertia typically by a factor of 1.5, implying amplitudes lower by about 20% (see Eqs. 35, 34). In the  $(1, -1)$  case we may have the opposite situation if  $\Omega > \Delta\omega$ .

Excitation of nonradial modes provides a natural explanation of basic properties of the Blazhko-type modulation. Of course, our simple treatment of non-linear effects precludes a detailed comparison with observations. The basic characteristics of the modulation are periods and ranges of amplitude variation.

## 7.2 Comparison with Observational Data

We are now in the position to compare quantitative prediction of our model with observational data on the Blazhko effect. The numbers to compare are modulation periods and ranges of amplitude modulation.

The modulation to pulsation period ratio,  $P_B/P_0$ , ranges from 20 to 1000 (Kovács 1993). In our model we have

$$\frac{P_B}{P_0} = \frac{2\omega_0}{\Delta\omega} \frac{1}{|\Omega/\Delta\omega + k|}, \quad (90)$$

where  $\Delta\omega$  is the frequency difference between centroids of multiplets of radial orders  $n$  and  $n+1$ . We set  $k=0$  in the case of modes from the same multiplet and  $k=m_n$  in the case of modes from the consecutive multiplets. From Fig. 6 of DC we find the values of  $\Delta\omega/\omega_0$  for the  $l=1$  modes in the vicinity of the fundamental mode ranging from 4.5 to  $7.5 \times 10^{-3}$ . Let us consider first the case  $k \neq 0$  and  $\Omega \ll \Delta\omega$ . Then we find  $270 < P_B/P_0 < 450$ . Unless our models of RR Lyr stars are grossly inadequate, we cannot account for large fraction of observed modulation periods. Interpretation of Blazhko stars with short modulation periods demands  $\Omega \gg \Delta\omega$ .

We are not aware of any  $V_{\text{rot}} \sin i$  determination for any RR Lyr star. Peterson *et al.* (1996) provide only an upper limit of 10 km/s for 8 RRab stars. If we assume uniform rotation we may translate this upper limit to the minimum value of  $P_B/P_0$ . This minimum value is about 30. This is still more than the lowest observed modulation period. However, we should remind that  $\Omega$  does not refer to the surface but to the deep interior and it is quite plausible that the interior rotates much faster than the surface. We conclude that our prediction of modulation periods is not inconsistent with observations.

A comparison of our prediction regarding ranges of amplitude modulation with observational data is much more complicated. Firstly, inadequacy of our approximation is certainly far more important in this case; secondly, we have much less observational information. The only systematic survey of amplitude modulation in RR Lyr stars is that from the MACHO project (Alcock *et al.* 2000), but it is restricted to RRc stars in LMC. Let us remind that the Blazhko phenomenon is much more common in RRab stars than in RRc. In Alcock's *et al.* (2000) list we find the cases of rather different side peak amplitudes, much larger than those implied by our Eq. (64). Also there are cases of side peak amplitudes exceeding the central peak amplitude, contrary to our predictions. We believe, however, that these cases do not invalidate the very essence of our model, but point out to necessity of supplementing it by taking into account more interacting modes. Samples of Blazhko RRab stars from the MACHO project were analyzed by Kurtz *et al.* (2000). In a few examples they point out different degrees of phase and amplitude modulations. Our model provides a natural explanation of the above diversity.

For a comparison of our simplified theory with observations, the radial velocity data are more suitable. The reason is that the higher order nonlinear effects, which we ignored, are more important in light than in radius variations. Unfortunately, the radial velocity data on Blazhko phenomenon are very limited. Recently, Chadid *et al.* (1999) investigated line profile variations in RR Lyr itself. They find a triplet associated with the main frequency but it is not exactly equally spaced. The spacings are 0.027, 0.020 c/d. We do not know whether this departure from equidistance is significant. The relative side peak

amplitudes are about 0.3 which is about the maximum value predicted by our model.

## 8 Conclusions and Discussion

We solved simplified amplitude equations describing resonant coupling between radial and nonradial modes. The equations cover the case of 1:1 resonance between a radial and an axisymmetric ( $m=0$ ) nonradial mode as well as the case of 2:1+1 resonance between a radial mode and a  $(m, -m)$  pair. We showed that in the limit of slow rotation and modes of the same multiplet the two cases are equivalent. If the modes belong to neighboring multiplets this is not true, but the treatment is very similar. The crucial parameter is  $\Delta\omega$  which is a measure of the departure from exact resonance. We showed that if radial pulsations are unstable, which requires  $\Delta\omega$  to be less than certain critical value, then there are typically two branches of stationary solutions which merge at  $\Delta\omega=0$ . The branch corresponding to lower relative amplitude of the nonradial mode is almost always stable. The other branch may also be stable in a certain range around  $\Delta\omega=0$ , but the region of attraction to solutions in the latter branch is relatively small. For this reason we use the solutions corresponding to  $\Delta\omega=0$  as representing the maximum departure from pure radial pulsation.

Excitation of an axisymmetric nonradial mode leads to pulsation with constant amplitude. The presence of a nonradial component affects both period and amplitude. The most significant effect is an amplitude change in the case of excitation of a dipole mode. The size of the expected amplitude change depends on  $\Delta\omega$  and the aspect angle of the pulsation axis. Both must be regarded as random quantities. The former, in principle, is determined by stellar parameters, but it is so sensitive that we may specify only its upper limit which is  $(\omega_{n,l} - \omega_{n+1,l})/2$ . We found that for the specified model and pulsation mode the uncertainty of the amplitude may reach up to 40%. The consequence is that pulsation amplitude and other characteristics of light curve are not uniquely determined by mean stellar parameters. This is not a good news for diagnostic applications of the light curve data.

Amplitude modulated pulsation is expected in the case of excitation of non-axisymmetric pair of nonradial modes of low degree  $l$ . Here again the case of  $l=1$  is most likely and most interesting. In this case we find that the maximum range of amplitude modulation is about 40%. The modulation period is determined by the characteristic of the deepest layers of the radiative stellar interior. Specifically, it is given by  $4\pi/|\Omega_{\text{rot}} + k(\omega_{n,l} - \omega_{n+1,l})|$ , where  $k=0, \pm 1$ ,  $\Omega_{\text{rot}}$  is the mean rotation rate in those layers, and  $\omega_{n,l} - \omega_{n+1,l}$  is the distance between the centers of the consecutive multiplets,  $n$  at fixed  $l$ . Hence, if this is the modulation seen as the Blazhko effect then the Blazhko period is a probe of deep interior properties of Horizontal Branch stars. The prospect of sounding interiors of HB stars is quite interesting.

The reader must be reminded of simplifications used in this paper. We rely on the formalism which assumes that the amplitudes are small. This is not

true. Especially our prediction of the light amplitude must be regarded unreliable. Higher order nonlinear effects should be included. Our treatment of mode coupling was simplified by adopting a simple scaling of the coefficients and by assuming that they are either pure real or pure imaginary. Taking into account their complex character may imply an instability of constant amplitude solution and imply periodic limit cycle (Moskalik 1986). In this case, the modulation period would be determined by the properties of the outermost layers. Validity of our formalism is restricted to the cases of 1:1 and 2:1+1 resonances. Furthermore, couplings which are not covered by our formalism may also play a role. These include coupling between the nonradial modes within the multiplet as well as the coupling between the radial mode and two axisymmetric nonradial modes of consecutive multiplets. We plan to consider these cases in our subsequent paper.

We have realized that there is a considerable paucity of observational data on the Blazhko effect. The crucial signature of the type of mode coupling considered in this paper is the occurrence of the equidistant triplet in pulsation spectra. Such spectra, based on modern photometry of RR Lyr stars, are available only for RRc stars and not for RRab stars, for which the Blazhko effect is claimed to be much more common. From the point of view of testing our model of the Blazhko effect, spectroscopy is more suitable for detecting nonradial modes than photometry. Further, if such modes are detected we may extract the information about mode order and the aspect angle of the pulsation axis. With this information we may learn about differential rotation in the interiors of Horizontal Branch stars. Spectroscopic studies of Blazhko effect began only very recently (Chadid *et al.* 1999).

**Acknowledgements.** This work was supported in part by the KBN grant 2-P03D-14.

## REFERENCES

- Aerts, C., and Eyer, L. 2000, "Delta Scuti and Related Stars", *ASP Conf. Ser.*, 210, Eds. M. Breger and M. Montgomery, p. 113.
- Alcock, C., *et al.* 2000, *Astrophys. J.*, **542**, 257.
- Blazhko, S. 1907, *Astron. Nachr.*, **175**, 325.
- Buchler, J.R., and Goupil, M.J. 1984, *Astrophys. J.*, **279**, 394.
- Buchler, J.R., Goupil, M.J., and Hansen, C.J. 1997, *Astron. Astrophys.*, **321**, 159.
- Buchler, J.R., Goupil, M.J., and Serre, T. 1995, *Astron. Astrophys.*, **296**, 405.
- Chadid, M., Kolenberg, K., Aerts, C., and Gillet, D. 1999, *Astron. Astrophys.*, **352**, 201.
- Dziembowski, W.A. 1977a, *Acta Astron.*, **27**, 95.
- Dziembowski, W.A. 1977b, *Acta Astron.*, **27**, 203.
- Dziembowski, W.A. 1982, *Acta Astron.*, **32**, 147.
- Dziembowski, W.A., and Cassisi, S. 1999, *Acta Astron.*, **49**, 371.
- Dziembowski, W.A., and Królikowska, M. 1985, *Acta Astron.*, **35**, 5.
- Garrido, R. 2000, "Delta Scuti and Related Stars", *ASP Conf. Ser.*, 210, Eds. M. Breger and M. Montgomery, p. 67.
- Jurcsik, J., and Kovács, G. 1996, *Astron. Astrophys.*, **312**, 111.
- Kovács, G. 1993, "Stochastic Processes in Astrophysics", *Annals of New York Academy of Sciences*, 706, Eds. J.R. Buchler and H.E. Kandrups, p. 70.



- Kovács, G. 2000, "Nonlinear Studies of Stellar Pulsation", Eds. M. Takeuti and D.D. Sasselov, *Astrophysics and Space Science Library Series*, Kluwer (in press).
- Kovács, G., and Buchler, J.R. 1988, *Astrophys. J.*, **324**, 1026.
- Kovács, G., and Jurcsik, J. 1996, *Astrophys. J. Letters*, **466**, L17.
- Kurtz, D.W., *et al.* 2000, "The Impact of Large-Scale Surveys on Pulsating Star Research", *ASP Conf. Ser.*, 203, Eds. L. Szabados and D. Kurtz, p. 291.
- Moskalik, P. 1986, *Acta Astron.*, **36**, 333.
- Osaki, Y. 1977, *PASJ*, **29**, 234.
- Peterson, R.C., Carney, B.W., and Latham D.W. 1996, *Astrophys. J. Letters*, **465**, L47.
- Shibahashi, H. 1995, in: "GONG'94: Helio- and Asteroseismology", *ASP Conf. Ser.*, Vol. 76, Eds. R.K. Ulrich, E.J. Rhodes, Jr., and W. Dáppen, p. 618.
- Shibahashi, H. 2000, "The Impact of Large-Scale Surveys on Pulsating Star Research", *ASP Conf. Ser.*, 203, Eds. L. Szabados and D. Kurtz, p. 299.
- Szeidl, B. 1988, "Multimode Stellar Pulsations", Eds. G. Kovács, L. Szabados, B. Szeidl, Konkoly Observatory, Kultura, Budapest, p. 45.
- Unno, W., Osaki, Y., Saio, H., and Shibahashi, H. 1989, "Nonradial Oscillations of Stars", University of Tokyo Press.
- Van Hoolst, T. 1992, "Nonlinear, Nonradial Oscillations of Stars. Resonances Between Two Modes with Nearly Equal Frequencies", PhD thesis, Katholieke Universiteit, Leuven.
- Van Hoolst, T. 1994, *Astron. Astrophys.*, **292**, 471.
- Van Hoolst, T., Dziembowski, W.A., and Kawaler, S.D. 1998, *MNRAS*, **297**, 536.
- Van Hoolst, T., and Waelkens, C. 1995, *Astron. Astrophys.*, **295**, 361.
- Wersinger, J.M., Finn, J.M., and Ott, E. 1980, *Physics of Fluids*, **23**, 1142.

## Appendix

### A Amplitude Equations for Two- and Three-Mode Resonance

In this Appendix we outline the derivation of amplitude equations for the 1:1 resonance (the radial and the  $m=0$  nonradial mode) and the 2:1+1 resonance (the radial and the pair  $\pm m$  of nonradial modes). We briefly sketch how the basic form of amplitude equations and the relations between coupling coefficients can be obtained. Our main aim is to capture the difference in the coupling coefficients for both cases by considering typical third order terms.

The oscillatory mode is described by the displacement given in Eq. (4). The nonlinear equations for the mode amplitudes contain operators acting on eigenfunctions and integrated over the volume of a star. For simplicity we will be concerned only with the radial component of the displacement. Taking into account angular components introduces additional terms in integrals but does not change the form of the equations and the relations between coefficients. Thus we can write

$$\xi_{r,j}(\mathbf{r}, t) = \frac{1}{2} a_j(t) w_j(\mathbf{r}, t) + cc, \quad (A1)$$

where

$$w_j(\mathbf{r}, t) = h_j(r) Y_l^m(\theta, \phi) e^{i\omega_j t}. \quad (A2)$$

Degrees  $l, m$  correspond to mode  $j$ . Spherical harmonics are expressed by the

normalized associated Legendre functions

$$Y_l^m(\theta, \phi) = (-1)^m \frac{1}{\sqrt{2\pi}} \tilde{P}_{l,m}(\cos\theta) e^{im\phi}, \quad (A3)$$

$$\tilde{P}_{l,m}(x) = \sqrt{\frac{(2l+1)(l-m)!}{2(l+m)!}} P_{l,m}(x), \quad (A4)$$

and

$$P_{l,m}(x) = \frac{1}{2^l l!} (1-x^2)^{m/2} \frac{d^{l+m}}{dx^{l+m}} (x^2-1)^l \quad (A5)$$

is the associated Legendre function. Normalizations are

$$\int |Y_{l,m}|^2 d\Omega = 1, \quad (A6)$$

$$\int_{-1}^1 \tilde{P}_{l,m}^2(x) dx = 1. \quad (A7)$$

We will assume the dominant nonlinear terms to be of the third order. These terms in equation for the time derivative of the amplitude  $a_j$  are determined by the expression

$$T_j = \frac{1}{I_j} \langle w_j | N | \xi_1, \xi_2, \xi_3 \rangle, \quad (A8)$$

where  $I_j$  is the mode inertia,  $N$  is some operator that is linear with respect to each argument and symmetrical with respect to interchanges of arguments and 1, 2, 3 correspond to all modes that gives nonvanishing resonant terms. The bracket denotes integration over the volume of the star. The operator in Eq. (A8) can be presented in the form

$$\begin{aligned} \langle w_j | N | \xi_1, \xi_2, \xi_3 \rangle &= \\ &= a_1 a_2 a_3 \langle h_j | N_T | h_1, h_2, h_3 \rangle \langle Y_j | N_{\theta, \varphi} | Y_1, Y_2, Y_3 \rangle e^{i(\omega_1 + \omega_2 + \omega_3 - \omega_j)t}. \end{aligned} \quad (A9)$$

The angular part of the operator may be simplified to the factor  $\int Y_j^* Y_1 Y_2 Y_3 d\Omega$ .

We keep only resonant terms, *i.e.*, terms slowly varying or constant in time. This means one of the frequencies  $\omega_1, \omega_2, \omega_3$  has to be taken with minus sign, which implies one of the eigenfunctions  $\xi_1, \xi_2, \xi_3$  should be taken complex conjugated. Additionally, integration of the product of spherical harmonics includes integration of factor  $\exp[i\varphi(m_1 + m_2 + m_3 - m_j)]$  where one of the numbers  $m_1, m_2, m_3$  is taken with negative sign (complex conjugation of spherical harmonic) and for nonvanishing terms the sum of  $m$ 's in the exponent has to be zero.

### A.1 The 1:1 Resonance

The nonvanishing terms are

$$\begin{aligned} \langle w_0|N|\xi_0, \xi_0, \xi_0^* \rangle + \langle w_0|N|\xi_0, \xi_0^*, \xi_0 \rangle + \langle w_0|N|\xi_0^*, \xi_0, \xi_0 \rangle = \\ = 3\langle h_0|N_r|h_0, h_0, h_0^* \rangle \int (Y_0^* Y_0)^2 d\Omega |a_0|^2 a_0, \end{aligned} \quad (\text{A10})$$

and similarly

$$\begin{aligned} \langle w_0|N|\xi_0, \xi_l, \xi_l^* \rangle + \text{permutations} = \\ = 6\langle h_0|N_r|h_0, h_l, h_l^* \rangle \int |Y_0|^2 |Y_l|^2 d\Omega |a_l|^2 a_0, \end{aligned} \quad (\text{A11})$$

$$\begin{aligned} \langle w_0|N|\xi_0^*, \xi_l, \xi_l \rangle + \text{permutations} = \\ = 3\langle h_0|N_r|h_0^*, h_l, h_l \rangle \int (Y_0^*)^2 Y_l^2 d\Omega e^{2it(\omega_l - \omega_0)} a_l^2 a_0^*. \end{aligned} \quad (\text{A12})$$

All  $m$ 's are equal to zero. For even  $l$  terms involving  $\int Y_l^3$  do not vanish, but we neglect them as was explained in Section 3.1. Symmetrically

$$\begin{aligned} \langle w_l|N|\xi_l, \xi_l, \xi_l^* \rangle + \text{permutations} = \\ = 3\langle h_l|N_r|h_l, h_l, h_l^* \rangle \int (Y_l Y_l^*)^2 d\Omega |a_l|^2 a_l, \end{aligned} \quad (\text{A13})$$

$$\begin{aligned} \langle w_l|N|\xi_l, \xi_0, \xi_0^* \rangle + \text{permutations} = \\ = 6\langle h_l|N_r|h_l, h_0, h_0^* \rangle \int |Y_0|^2 |Y_l|^2 d\Omega |a_0|^2 a_l, \end{aligned} \quad (\text{A14})$$

$$\begin{aligned} \langle w_l|N|\xi_l^*, \xi_0, \xi_0 \rangle + \text{permutations} = \\ = 3\langle h_l|N_r|h_l^*, h_0, h_0 \rangle \int Y_0^2 (Y_l^*)^2 d\Omega e^{-2it(\omega_l - \omega_0)} a_0^2 a_l^*. \end{aligned} \quad (\text{A15})$$

Radial integration may be done only over the envelope. The justification of it is that the radial mode eigenfunction is nearly zero in the interior and most terms involve it. The term involving only the nonradial mode eigenfunction is the saturation term and we are interested only in its real part, as was explained in Section 3.1. The real parts of saturation terms are determined by nonadiabaticity of oscillations which is very weak in the deep interior and it is sufficient to restrict integration to nonadiabatic envelope. But in the envelope all radial eigenfunctions are nearly the same. It means the brackets on the right-hand sides of Eqs. (A10)–(A15) are the same.

Let us introduce the quantities

$$J_{00} = 3\langle h_0|N_r|h_0, h_0, h_0\rangle \int Y_0^4 d\Omega = \frac{3}{4\pi} \langle h_0|N_r|h_0, h_0, h_0\rangle, \quad (\text{A16})$$

$$J_{0l} = 3\langle h_0|N_r|h_0, h_l, h_l\rangle \int Y_0^2 Y_l^2 d\Omega = \frac{3}{4\pi} \langle h_0|N_r|h_0, h_0, h_0\rangle = J_{00}, \quad (\text{A17})$$

$$\begin{aligned} J_{ll} &= 3\langle h_l|N_r|h_l, h_l, h_l\rangle \int Y_l^4 d\Omega = \\ &= \frac{3}{2\pi} \langle h_0|N_r|h_0, h_0, h_0\rangle \int_{-1}^1 \tilde{P}_l^4(x) dx = 2J_{00}H_l, \end{aligned} \quad (\text{A18})$$

where we used normalization of spherical harmonics, the fact that they are real,  $h_0(r) = h_l(r)$  in the envelope, and the easy-to-show property

$$\int Y_1 Y_2 Y_3 Y_4 d\Omega = \frac{1}{2\pi} \int_{-1}^1 \tilde{P}_1 \tilde{P}_2 \tilde{P}_3 \tilde{P}_4 dx.$$

The quantity  $H_l$  is equal  $\int_{-1}^1 \tilde{P}_l^4(x) dx$ . With Eqs. (A16)–(A18) one can write more explicit expressions for the nonlinear terms (A8)

$$I_0 T_0 = J_{00}|a_0|^2 a_0 + 2J_{00}|a_l|^2 a_0 + J_{00} a_l^2 a_0^* e^{2i(\omega_l - \omega_0)t}, \quad (\text{A19})$$

$$I_l T_l = 2J_{00}|a_0|^2 a_l + 2J_{00}H_l|a_l|^2 a_l + J_{00} a_0^2 a_l^* e^{-2i(\omega_l - \omega_0)t}. \quad (\text{A20})$$

With above expressions the amplitude equations are

$$\frac{da_0}{dt} = \kappa_0 a_0 + T_0, \quad (\text{A21})$$

$$\frac{da_l}{dt} = \kappa_l a_l + T_l. \quad (\text{A22})$$

Relations given by Eq. (13) and the scaling-with-inertia properties (Eqs. 14 and 15) are obtained in a straightforward manner from Eqs. (A19) and (A20).

## A.2 The 2:1+1 Resonance

In this case we have nonvanishing resonant terms

$$\langle w_0|N|\xi_0, \xi_0, \xi_0^*\rangle : 3 \text{ permutations,}$$

$$\langle w_0|N|\xi_0, \xi_+, \xi_+^*\rangle : 6 \text{ permutations,}$$

$$\langle w_0|N|\xi_0, \xi_-, \xi_-^*\rangle : 6 \text{ permutations,}$$

$$\langle w_0|N|\xi_0^*, \xi_+, \xi_-\rangle : 6 \text{ permutations,}$$

$$\langle w_+|N|\xi_+, \xi_+, \xi_+^*\rangle : 3 \text{ permutations,}$$

$$\langle w_+|N|\xi_+, \xi_0, \xi_0^*\rangle : 6 \text{ permutations,}$$

$$\langle w_+|N|\xi_+, \xi_-, \xi_-^*\rangle : 6 \text{ permutations,}$$

$$\langle w_+|N|\xi_-^*, \xi_0, \xi_0\rangle : 3 \text{ permutations,}$$

and symmetrically for the mode ‘-’. All properties of the radial eigenfunctions are the same as in the previous case. The only  $m$ -dependent quantities are eigenfrequencies and spherical harmonics. Then quantities given by Eqs. (A16)–(A18) are defined analogically, but the product  $Y_l^m Y_l^{-m}$  should be used instead of  $Y_l^2$ . Quantity  $J_{00}$  is the same as in the  $m=0$  case, as well as  $J_{0l}^m$  which is equal  $J_{00}$ , too. Finally,  $J_{ll}^m = 2J_{00}H_l^m$ , where  $H_l^m = \int_{-1}^1 \tilde{P}_{l,m}^A(x)dx$ . Then the nonlinear terms (A8) are

$$\begin{aligned} I_0 T_0 &= J_{00}|a_0|^2 a_0 + 2J_{00}(|a_+|^2 + |a_-|^2) a_0 + \\ &\quad + 2J_{00} a_- a_+ a_0^* e^{i(\omega_+ + \omega_- - 2\omega_0)t}, \end{aligned} \quad (A23)$$

$$\begin{aligned} I_{\pm} T_{\pm} &= 2J_{00}|a_0|^2 a_{\pm} + 2J_{00}H_l^m(|a_{\pm}|^2 + 2|a_{\mp}|^2) a_{\pm} + \\ &\quad + J_{00} a_0^2 a_{\mp}^* e^{-i(\omega_+ + \omega_- - 2\omega_0)t}. \end{aligned} \quad (A24)$$

When we assume equality of nonradial modes inertia, which implies Eq. (24), we obtain, similarly as in the previous case, Eqs. (25)–(30).

## B Observed Radial Velocity and Light Curves

We use here a simple analytical expressions (Dziembowski 1977) which should be sufficient for crude estimates presented in this paper. The expression for observable radial velocity due to an individual oscillation mode is given by

$$V_{\text{rad}} = \omega_{l,m} R_{\text{ph}} A_{l,m} \tilde{P}_{l,m}(\cos \Theta_0) \cos(\omega_{l,m} t - \pi/2 - m\Phi_0) (u_l + \alpha_H v_l) \quad (B1)$$

where  $l, m$  are quantum numbers of the mode;  $\omega_{l,m}$  is its frequency;  $R_{\text{ph}}$  is the photospheric stellar radius;  $A_{l,m}$  and  $\tilde{P}_{l,m}$  are mode amplitude and the normalized associated Legendre function, respectively;  $\Theta_0, \Phi_0$  determine the direction to the observer in the system of coordinates connected with the star;  $u_l, v_l$  are certain limb darkening dependent quantities which take into account averaging over the stellar disc; and  $\alpha_H = GM/(\omega^2 R_{\text{ph}}^3)$ . For RR Lyr stars this quantity is of the order of 0.1. Similarly we have the expression for the bolometric magnitude change

$$\begin{aligned} \Delta M_{\text{bol}} &= -1.086 A_{l,m} \tilde{P}_{l,m}(\cos \Theta_0) [f_l \cos(\omega_{l,m} t + \psi_l - m\Phi_0) b_l + \\ &\quad + \cos(\omega_{l,m} t - m\Phi_0) (2b_l - c_l)] \end{aligned} \quad (B2)$$

where  $b_l, c_l$  are again certain limb darkening dependent integrals over the stellar disc. Quantities  $f_l, \psi_l$  are obtained with solving nonadiabatic oscillation equations. They allow us to translate the radius changes into the luminosity changes. The first term in the square bracket in Eq. (B2) describes emerging flux oscillations while the second term describes the radius changes connected with oscillatory mode. The values of  $b_l, c_l, u_l, v_l$  are given by Dziembowski (1977b) for Eddington’s limb darkening law. For  $l > 2$  they are small due to the averaging

effect. The highest values are obviously for  $l=1$  and for radial modes and we focus on these modes. Then we have

$$\begin{aligned}\tilde{P}_{0,0} &= \sqrt{1/2}, & \tilde{P}_{1,0}(\cos \Theta_0) &= \sqrt{3/2} \cos \Theta_0, \\ \tilde{P}_{1,1}(\cos \Theta_0) &= \sqrt{3/4} \sin \Theta_0.\end{aligned}$$

The averaging coefficients are  $u_0 = 0.708$ ,  $u_1 = 0.55$ ,  $v_0 = 0$ ,  $v_1 = 0.45$ ,  $b_0 = 1$ ,  $b_1 = 0.708$ ,  $c_0 = 0$ , and  $c_1 = 1.416$ . Since  $\alpha_H$  is small we will neglect terms  $\alpha_H v_l$ .

## B.1 The 1:1 Resonance

Let us consider a superposition of a radial and a  $m=0$  nonradial resonant modes satisfying the double-mode fixed-point solution of AEs. Then their real frequencies are exactly equal due to the phase-lock phenomenon. The relative phase  $\Gamma$  is given by Eq. (12) and we see that for phase-locked solution we have

$$\Gamma = 2(\phi_{l,0} - \phi_{0,0})$$

where  $\phi_{j,0}$  are initial phases in the expression

$$\phi_j = \frac{d\phi_j}{dt}t + \phi_{j,0}.$$

For individual mode the time dependence is given by  $\cos(\omega_j^l t + \phi_j) = \cos(\omega_j t + \phi_{j,0})$ , where  $\omega_j^l$  and  $\omega_j$  are the linear and nonlinear frequencies, respectively. We may choose the initial phase  $\phi_{0,0}$  to be zero. Then we have  $\phi_{j,0} = \Gamma/2$  and with the use of Eq. (B1) for  $(l, m) = (0, 0)$  and  $(l, 0)$ , we get

$$\begin{aligned}V_{\text{rad}} &= A_0 \omega_0 R_{ph} u_0 \tilde{P}_{0,0} \cos(\omega_0 t - \pi/2) + \\ &\quad + A_l \omega_l R_{ph} u_l \tilde{P}_{l,0}(\cos \Theta_0) \cos(\omega_l t - \pi/2 + \Gamma/2) = \\ &= A_0 \omega R_{ph} \tilde{P}_{0,0} u_0 [\cos(\omega t - \pi/2) + \epsilon_v \cos(\omega t - \pi/2 + \Gamma/2)],\end{aligned}\quad (B3)$$

where we adopted  $\omega_0 = \omega_l \equiv \omega$  and introduced

$$\epsilon_v = \frac{\tilde{P}_{l,0}(\cos \Theta_0) u_l A_l}{\tilde{P}_{0,0} u_0 A_0}.\quad (B4)$$

Eq. (B3) may be written in the form

$$\begin{aligned}V_{\text{rad}} &= A_{v,0} [\cos(\omega t - \pi/2) (1 + \epsilon_v \cos(\Gamma/2)) - \epsilon_v \sin(\Gamma/2) \sin(\omega t - \pi/2)] = \\ &= A_{v,0} p \cos(\omega t - \pi/2 + \varphi)\end{aligned}\quad (B5)$$

where

$$A_{v,0} = A_0 \omega R_{ph} u_0 \tilde{P}_{0,0}\quad (B6)$$

is the radial velocity amplitude for the radial mode,

$$p \cos \varphi = 1 + \epsilon_v \cos(\Gamma/2)\quad (B7)$$

and

$$p \sin \varphi = \epsilon_v \sin(\Gamma/2). \quad (B8)$$

From Eqs. (B5), (B7), and (B8) we see that the radial velocity amplitude is given by

$$A_v = A_{v,0} \sqrt{1 + \epsilon_v^2 + 2\epsilon_v \cos(\Gamma/2)}, \quad (B9)$$

which is equivalent to Eq. (72).

With the same choice of phases  $\phi_{j,0}$  we obtain for the bolometric magnitude variations

$$\begin{aligned} \Delta M_{\text{bol}} &= CA_0 \tilde{P}_{0,0} [f_0 \cos(\omega t + \psi_0) b_0 + \cos \omega t (2b_0 - c_0)] + \\ &\quad + CA_1 \tilde{P}_{1,0} (\cos \Theta_0) f_1 b_1 \cos(\omega t + \psi_1 + \Gamma/2) = \\ &= CA_0 \tilde{P}_{0,0} f \left[ \frac{2}{f} \cos \omega t + \cos(\omega t + \psi) + \epsilon_M \cos(\omega t + \psi + \Gamma/2) \right], \end{aligned} \quad (B10)$$

where, after Dziembowski (1997b), we assume  $f_l = f_0 \equiv f$  and  $\psi_l = \psi_0 \equiv \psi$ , for our low degree modes. The quantity  $\epsilon_M$  is defined in the same way as  $\epsilon_v$  but with  $b_l$  instead of  $u_l$ . The radius changes vanish for  $l=1$  modes. The contribution to light variation from the radial mode is given by

$$\Delta M_{\text{bol},0} = A_{M\text{bol},0} \cos(\omega t + \varphi_0) \quad (B11)$$

where

$$A_{M\text{bol},0} = CA_0 \tilde{P}_{0,0} f p_0, \quad (B12)$$

$$p_0 \cos \varphi_0 = \frac{2}{f} + \cos \psi, \quad (B13)$$

$$p_0 \sin \varphi_0 = \sin \psi, \quad (B14)$$

and

$$p_0^2 = 1 + \frac{4}{f^2} + \frac{4}{f} \cos \psi. \quad (B15)$$

After adding the contribution from the nonradial mode we obtain

$$\begin{aligned} \Delta M_{\text{bol}} &= CA_0 \tilde{P}_{0,0} f \{ \cos \omega t [p_0 \cos \varphi_0 + \epsilon_M \cos(\psi + \Gamma/2)] - \\ &\quad - \sin \omega t [p_0 \sin \varphi_0 + \epsilon_M \sin(\psi + \Gamma/2)] \} = \\ &= CA_0 \tilde{P}_{0,0} f p_1 \cos(\omega t + \varphi_1) = A_{M\text{bol}} \cos(\omega t + \varphi_1), \end{aligned} \quad (B16)$$

where

$$p_1 \cos \varphi_1 = p_0 \cos \varphi_0 + \epsilon_M \cos(\psi + \Gamma/2), \quad (B17)$$

$$p_1 \sin \varphi_1 = p_0 \sin \varphi_0 + \epsilon_M \sin(\psi + \Gamma/2), \quad (B18)$$

and

$$A_{M\text{bol}} = CA_0 \tilde{P}_{0,0} f p_1. \quad (B19)$$

Eqs. (B13), (B14), (B17), and (B18) yield

$$p_1^2 = p_0^2 + \epsilon_M^2 + 2\epsilon_M \left[ \frac{2}{f} \cos(\psi + \Gamma/2) + \cos(\Gamma/2) \right]. \quad (B20)$$

Using Eqs. (B12), (B19), and (B20) we see that the presence of nonradial mode changes the observed amplitude by the factor

$$\frac{p_1}{p_0} = \sqrt{1 + \frac{\epsilon_M^2}{p_0^2} + \frac{2\epsilon_M}{p_0^2} \left[ \frac{2}{f} \cos(\psi + \Gamma/2) + \cos(\Gamma/2) \right]}. \quad (B21)$$

This equation is equivalent to Eq. (74).

## B.2 The 2:1+1 Resonance

We consider here a superposition of a radial mode and a pair of nonradial modes. The phase-lock phenomenon in this case causes the three frequencies to be equidistant, with the radial mode frequency in the center. The relative phase  $\Gamma$  is given by Eq. (23) and, similarly as in Appendix B.1, for the constant amplitude solution, it is given by

$$\Gamma = \phi_{m,0} + \phi_{-m,0} - 2\phi_{0,0}.$$

Again we choose  $\phi_{0,0} = 0$ . We denote amplitudes and resonant frequencies of the radial, the  $(l, m)$ , and  $(l, -m)$  modes as  $A_0$ ,  $A_-$ ,  $A_+$ , and  $\omega$ ,  $\omega - \lambda$ ,  $\omega + \lambda$ , respectively. Now we have

$$\begin{aligned} V_{rad}^m &= A_0 \omega R_{ph} u_0 \tilde{P}_{0,0} \cos(\omega t - \pi/2) + \\ &\quad + A_- (\omega - \lambda) R_{ph} u_l \tilde{P}_{l,m}(\cos \Theta_0) \cos(\omega t - \lambda t - \pi/2 + \phi_{m,0}) + \\ &\quad + A_+ (\omega + \lambda) R_{ph} u_l \tilde{P}_{l,m}(\cos \Theta_0) \cos(\omega t + \lambda t - \pi/2 + \phi_{-m,0}) = \\ &= A_{v,0} [\cos(\omega t - \pi/2) + \epsilon_{v,-} \cos(\omega t - \lambda t - \pi/2 + \phi_{-,0}) + \\ &\quad + \epsilon_{v,+} \cos(\omega t + \lambda t - \pi/2 + \phi_{+,0})] \end{aligned} \quad (B22)$$

where

$$\epsilon_{v,\pm} = \frac{A_{\pm}}{A_0} \frac{\omega \pm \lambda}{\omega} \frac{u_l}{u_0} \frac{\tilde{P}_{l,m}(\cos \Theta_0)}{\tilde{P}_{0,0}} \approx \frac{u_l}{u_0} \frac{\tilde{P}_{l,m}(\cos \Theta_0)}{\tilde{P}_{0,0}} \frac{A_{\pm}}{A_0}. \quad (B23)$$

We made use here of  $\lambda \ll \omega$ . The amplitude  $A_{v,0}$  is given in Eq. (B6). Keeping only linear terms in  $\epsilon_{v,\pm}$  and making use of certain well-known trigonometric relations we get

$$V_{rad}^m = A_{v,0} [1 + a \cos(\lambda t + \beta)] \cos(\omega t - \pi/2 + b \cos(\lambda t + \gamma)) \quad (B24)$$

where the modulation coefficients,  $a$ ,  $b$ , and the phase shifts,  $\beta$ ,  $\gamma$ , are given by

$$a \cos \beta = \epsilon_{v,-} \cos \phi_{-,0} + \epsilon_{v,+} \cos \phi_{+,0}, \quad (B25)$$

$$a \sin \beta = -\epsilon_{v,-} \sin \phi_{-,0} + \epsilon_{v,+} \sin \phi_{+,0}, \quad (B26)$$

$$b \sin \gamma = \epsilon_{v,-} \cos \phi_{-,0} - \epsilon_{v,+} \cos \phi_{+,0}, \quad (B27)$$

$$b \cos \gamma = \epsilon_{v,-} \sin \phi_{-,0} + \epsilon_{v,+} \sin \phi_{+,0}. \quad (B28)$$



For  $l=1$  and  $A_- = A_+ \equiv A_1/\sqrt{2}$  we obtain

$$\epsilon_{v,\pm} = \frac{\sqrt{3}}{2} \sin \Theta_0 \frac{u_1 A_1}{u_0 A_0} \equiv \frac{\epsilon_{v,m}}{2}. \quad (B29)$$

Inserting it to Eqs. (B25)–(B28) leads to

$$a \cos \beta = \frac{\epsilon_{v,m}}{2} (\cos \phi_{-,0} + \cos \phi_{+,0}) = \epsilon_{v,m} \cos(\Gamma/2) \cos(\Delta/2), \quad (B30)$$

$$a \sin \beta = \epsilon_{v,m} \cos(\Gamma/2) \sin(\Delta/2), \quad (B31)$$

$$b \sin \gamma = \epsilon_{v,m} \sin(\Gamma/2) \sin(\Delta/2), \quad (B32)$$

$$b \cos \gamma = \epsilon_{v,m} \sin(\Gamma/2) \cos(\Delta/2), \quad (B33)$$

where  $\Gamma = \phi_{+,0} + \phi_{-,0}$  and  $\Delta = \phi_{+,0} - \phi_{-,0}$ . Finally we get

$$a = \epsilon_{v,m} \cos(\Gamma/2), \quad (B34)$$

$$b = \epsilon_{v,m} \sin(\Gamma/2), \quad (B35)$$

$$\beta = \gamma = \Delta/2. \quad (B36)$$

Since the modulation frequency,  $\lambda$ , is much lower than the oscillation frequency,  $\omega$ , the choice of initial modulation phase is unimportant, and we may put  $\Delta=0$  in Eq. (B36) and thus get Eq. (79).

In a very similar manner we get the following expression for the bolometric light variations

$$\begin{aligned} \Delta M_{\text{bol}}^m = A_{M\text{bol},0} \{ & \cos \omega t [\cos \varphi_0 + \\ & + \frac{\cos \lambda t}{p_0} ( \cos \psi (\epsilon_{M,-} \cos \phi_{-,0} + \epsilon_{M,+} \cos \phi_{+,0}) - \\ & - \sin \psi (\epsilon_{M,-} \sin \phi_{-,0} + \epsilon_{M,+} \sin \phi_{+,0}) ) + \\ & + \frac{\sin \lambda t}{p_0} ( \cos \psi (\epsilon_{M,-} \sin \phi_{-,0} - \epsilon_{M,+} \sin \phi_{+,0}) + \\ & + \sin \psi (\epsilon_{M,-} \cos \phi_{-,0} - \epsilon_{M,+} \cos \phi_{+,0}) ) ] - \\ & - \sin \omega t [ \sin \varphi_0 + \\ & + \frac{\cos \lambda t}{p_0} ( \sin \psi (\epsilon_{M,-} \cos \phi_{-,0} + \epsilon_{M,+} \cos \phi_{+,0}) + \\ & + \cos \psi (\epsilon_{M,-} \sin \phi_{-,0} + \epsilon_{M,+} \sin \phi_{+,0}) ) + \\ & + \frac{\sin \lambda t}{p_0} ( \sin \psi (\epsilon_{M,-} \sin \phi_{-,0} - \epsilon_{M,+} \sin \phi_{+,0}) - \\ & - \cos \psi (\epsilon_{M,-} \cos \phi_{-,0} - \epsilon_{M,+} \cos \phi_{+,0}) ) ] \} \end{aligned} \quad (B37)$$

where  $A_{M\text{bol},0}$  is given by Eq. (B12),  $p_0, \varphi_0$  are given by Eqs. (B13), (B14), and

$$\epsilon_{M,\pm} = \sqrt{\frac{3}{2}} \sin \Theta_0 \frac{b_1 A_{\pm}}{b_0 A_0}. \quad (B38)$$

For  $\epsilon_{M,\pm} \ll 1$  we get approximately

$$\Delta M_{\text{bol}}^m = A_{M\text{bol},0} [1 + c \cos(\lambda t + \beta')] \cos(\omega t + \varphi_0 + d \cos(\lambda t + \gamma')) \quad (\text{B39})$$

where

$$\begin{aligned} p_0(c \cos \varphi_0 \cos \beta' - d \sin \varphi_0 \cos \gamma') &= \\ &= \epsilon_{M,-} \cos(\psi + \phi_{-,0}) + \epsilon_{M,+} \cos(\psi + \phi_{+,0}), \end{aligned} \quad (\text{B40})$$

$$\begin{aligned} p_0(-c \cos \varphi_0 \sin \beta' + d \sin \varphi_0 \sin \gamma') &= \\ &= \epsilon_{M,-} \sin(\psi + \phi_{-,0}) - \epsilon_{M,+} \sin(\psi + \phi_{+,0}), \end{aligned} \quad (\text{B41})$$

$$\begin{aligned} p_0(c \sin \varphi_0 \cos \beta' + d \cos \varphi_0 \cos \gamma') &= \\ &= \epsilon_{M,-} \sin(\psi + \phi_{-,0}) + \epsilon_{M,+} \sin(\psi + \phi_{+,0}), \end{aligned} \quad (\text{B42})$$

$$\begin{aligned} p_0(c \sin \varphi_0 \sin \beta' + d \cos \varphi_0 \sin \gamma') &= \\ &= \epsilon_{M,-} \cos(\psi + \phi_{-,0}) - \epsilon_{M,+} \cos(\psi + \phi_{+,0}). \end{aligned} \quad (\text{B43})$$

For  $A_+ = A_- \equiv A_1/\sqrt{2}$  we have again

$$\beta' = \gamma' = \Delta/2 \quad (\text{B44})$$

and then

$$c \cos \varphi_0 - d \sin \varphi_0 = \frac{\epsilon_{M,m}}{p_0} \cos(\psi + \Gamma/2), \quad (\text{B45})$$

$$c \sin \varphi_0 + d \cos \varphi_0 = \frac{\epsilon_{M,m}}{p_0} \sin(\psi + \Gamma/2) \quad (\text{B46})$$

where  $\epsilon_{M,m} \equiv 2\epsilon_{M,+} = 2\epsilon_{M,-}$ . The above equations lead to

$$c = \frac{\epsilon_{M,m}}{p_0} \cos(\psi + \Gamma/2 - \varphi_0), \quad (\text{B47})$$

$$d = \frac{\epsilon_{M,m}}{p_0} \sin(\psi + \Gamma/2 - \varphi_0). \quad (\text{B48})$$

Again choosing  $\Delta = 0$  in Eq. (B44) we obtain Eq. (B39) to be equivalent to Eq. (82)